POLITECNICO DI TORINO
Repository ISTITUZIONALE

Robust optimization of MTMD systems for the control of vibrations

Original
Robust optimization of MTMD systems for the control of vibrations / Pellizzari, F., Marano, G.C., Palmeri, A., Greco, R., Domaneschi, M.. - In: PROBABILISTIC ENGINEERING MECHANICS. - ISSN 0266-8920. - 70:(2022), p. 103347. [10.1016/j.probengmech.2022.103347]

Availability:
This version is available at: 11583/2970860 since: 2022-09-01T13:16:18Z

Publisher:
Elsevier

Published
DOI:10.1016/j.probengmech.2022.103347

Terms of use:

This article is made available under terms and conditions as specified in the corresponding bibliographic description in the repository

Publisher copyright
Elsevier postprint/Author's Accepted Manuscript

© 2022. This manuscript version is made available under the CC-BY-NC-ND 4.0 license
http://creativecommons.org/licenses/by-nc-nd/4.0/.The final authenticated version is available online at:
http://dx.doi.org/10.1016/j.probengmech.2022.103347

(Article begins on next page)

21 November 2026

Robust optimization of MTMD systems for the control of vibrations

F. Pellizzari[a], G.C. Marano[a], A. Palmeri[b], R. Greco[c], M. Domaneschi[a,*]

[a] *Department of Structural, Geotechnical and Building Engineering, Politecnico di Torino, Corso Duca degli Abruzzi, 24, 10129 Turin (TO) Italy*
[b] *School of Architecture, Building and Civil Engineering, Loughborough University, Loughborough LE11 3TU, UK*
[c] *Department of Civil, Environmental, Territory, Building and Chemical Engineering, Politecnico di Bari, Via Orabona 4, 70126, Bari, Italy*

Abstract

Multiple Tuned Mass Dampers (MTMD) is one of the simplest and most reliable solution to control the vibrations of a structure, e.g. allowing to deal with a wide distribution of structural natural frequencies and usually showing inherent stability. Nevertheless, uncertainties in the behavior of structures under random dynamic input may induce implications on the MTMD effectiveness, e.g. detuning or amplifications. Typically, uncertainties in the input are exclusively considered, while uncertainties affect as much also the mechanical parameters.

This paper proposes a robust optimum design of the MTMD, considering uncertainties both in the structural parameters and in the earthquake input. At this aim, a random vibration analysis of the response is adopted, and a direct linear perturbation method is applied on the uncertain parameters. Results show that a deterministic optimization is inappropriate for sensible systems as TMDs, while a robust optimization aims to better control the response with low computational efforts. Furthermore, the selection of the objective functions significantly affects the optimal design parameters, as the number of TMDs influences the robust designs.

Keywords: Robust Control, Optimization, MTMD, Earthquake, Uncertainties

*Corresponding author
Email address: marco.domaneschi@polito.it (M. Domaneschi)

1. Introduction

An important task in the field of structural optimization consists in the response assessment with dispersion of system parameters. Uncertainty of structural problems could attain many elements, which are considered deterministic in standard structural analysis, such as loads intensity or mechanical and geometrical configurations. A typically simplified approach assumes as the exclusive source of randomness the dynamic load as in case of earthquake or wind actions. The actions can be modeled by a stochastic process and the standard random vibration theory can be used [1]. Under these assumptions, a "conventional" stochastic structural optimization (CSSO) could be performed in the sense that, except for load nature, all the other parameters involved are assumed as deterministic.

The conception of vibration control using a mass damper dates back to 1909, when Frahm devised the "dynamic vibration absorber", a vibration control device. A single Tuned-Mass-Damper (TMD) can only control the vibration mode for which it was built, while another TMD can control a different mode. As a result, the notion of Multi-Tuned-Mass-Dampers (MTMD), which involves having a distinct TMD for each structural mode, seemed promising. Many studies in this field have focused on controlling a single mode, for example, different researchers have looked into a single-degree-of-freedom (SDF) structure-MTMD system with dampers' natural frequencies scattered over a range and a wide-band random input. For both robustness and response control, it was discovered that MTMD with natural frequencies dispersed around the structure's natural frequency can be more effective and resilient than a single TMD. Following that, the use of MTMD design to control multiple modes was examined in order to tune each damper to a specific mode, emphasizing the advantages of using such a control technique in decreasing structural response across a number of modes [2, 3, 4, 5]. The mitigation of flutter phenomena in bridge deck is one of the unique applications that has been researched for MTMD solutions [6, 7]. Com-

bining optimal damper adjustment with primary structure design for increased dynamic load performance has been also recently proposed for an innovative TMD solution, the Tuned-Mass-Damper-Inerter (TMDI) [8, 9].

In the field of random vibration, the first definition of structural optimal problem was proposed by Nigam [10], leading to a standard nonlinear restraint problem in which restraints were defined by probabilistic structural response indexes, while the objective function (OF) by structural weights. The use of a defined stochastic OF was later proposed for optimal damping design in the domain of seismic protection [11]. The optimal damping value of a device placed on the first story of a building was determined by minimizing an OF defined by the maximum structural displacement under white noise excitation. More recently, a specific and more complete stochastic approach has been proposed by Takewaki [12], in order to obtain a stiffness-damping simultaneous optimization of structural systems. The sum of mean square responses due to a stationary random excitation is minimized under constraints on total stiffness capacity and total damper capacity. An interesting alternative stochastic approach for optimum design of damping devices has been proposed by Park et al. [13] to minimize the total building life-cycle cost. It is based on a stochastic dynamic approach for failure probability evaluation, while the OF is defined in a deterministic way. The conventional stochastic optimization problem is also formulated by adopting the location and the amount of the viscous-elastic dampers as design variables [14]. Constraints are the maximum inter-storey drifts evaluated by the first crossing theory application in non-stationary conditions. Another interesting work regards unrestricted optimization of single nonlinear [15] and multiple linear [16] TMD by using as OF the structural displacement covariance of the protected system, and the input is treated as a simple stationary white noise. A complete stochastic CSSO is proposed by Marano et al. [17]. In this latter research, a based-optimum criterion is developed by adopting a covariance reliability approach, where both the OF and constraints are defined by a stochastic approach.

Contributions on seismic design assessment accounting for uncertainty in

seismic and structural modelling have been developed using different tools, including stochastic dynamics as well as statistical and probabilistic approaches in the context of performance-based earthquake engineering (PBEE). For example, a reliability based optimization of TMD parameters in seismic vibration control under bounded uncertain system parameters is proposed in [18]. The probability of failure of the system is used as the performance objective and the vibration control problem under bounded uncertainties is transformed to the appropriate deterministic optimization problems. More recently, Giaralis and Taflanidis [19] consider an optimum TMDI design framework accounting for parametric uncertainty to the host structure properties and to the seismic excitation. The probability of occurrence of different failure modes is adopted to quantify the structural performance, using as design objective function a linear combination of different performance variables (e.g., floor accelerations, interstory drifts. Li at al. [20] present robust design of a tuned mass damper (TMD) with hybrid stochastic excitation and epistemic uncertainties from the limited/insufficient knowledge of the structure and the site conditions. The worst performance indicators under the influences of uncertainties is used to approach and solve the optimization problem.

A recent state-of-the-art review on the response structural control by means of TMDs is recently presented in [21]. Specifically, the review considers various systems: i.e., single TMD, MTMDs, and spatially distributed MTMDs (d-MTMD). For the last two solutions, the review shows their effectiveness and robustness. Moreover, the paper presents as future research directions for systems protected by MTMDs those related to the evaluation of the effects of uncertainties in both stochastic input (e.g., for the seismic case) and structural parameters, both for time history and frequencies analysis. Indeed, contributions in this area currently appear limited to the case of Bhowmik and Debnath [22] where they consider the stochastic design of MTMDs with uncertainties.

The present research work aims to give a further contribution in this area by studying the robust optimal design of a MTMD solution, including uncertainties in both the input and the structural dynamics parameters, considering the effect

of a varying number of TMD devices, adopting different objective functions, comparing the results with the deterministic approach.

In detail, the applicability of the proposed robust optimization is shown by means of a MTMD device on a SDF system under earthquake input. Indeed, even if the structural analysis of a general N-dof system protected by more TMDs devices should be performed as an $N + n_{tmd}$ degrees of freedom (DOF) system, it can be observed that if the group of TMDs are tuned to the main structural frequency it is expected that its effectiveness is the greatest if an N degrees of freedom structural system oscillates around a predominant mode [23, 24]. Accordingly, it is reasonable considering only one main structural vibration mode, typically the first one, as descriptive of the protected element vibration for the MTMD optimal design. The MTMD is introduced in order to guarantee a suitable protection level in the primary structure for both the structure and its contents, towards a defined limit state.

The adopted SDF system is represented by a primary viscous-elastic system and it is subjected to a stationary filtered white noise stochastic process. The primary element is protected by a linear MTMD with varying number of devices against vibrations induced by base acceleration. It is assumed that uncertainty in problem parameters deals with primary system frequency and damping and base excitation spectral contents. The design vector (DV) here used contains the MTMD frequency and damping, and the ratio between the protected and the unprotected standard deviation of the main system displacements and absolute accelerations are used as OF.

An ordinary CSSO is performed for varying number of dampers to give a benchmark for the robust optimization, showing important implications that come from the chosen OF. The optimization of both performance and sensitivity deviation enters in the Multi Objective Optimization Problem class (MOOP). The robust solution is obtained by multi-objective criteria where optimization is achieved by minimizing both the OF mean value and standard deviation. Indeed, it is demonstrated that the design optimizes the structural reliability if also minimizes the robustness to uncertainty [25]. Mean and covariance OFs are

here obtained by applying the direct perturbation method (DPM) first-order approximation. A non-dominated sorting genetic algorithm (GA) in its second version (NSGA-II) (a Pareto-based multi-objective evolutionary algorithm) is used in order to evaluate the set of possible solutions. Finally, a comparison between deterministic and robust stochastic optimal solutions is shown.

2. Dynamic random vibrations analysis of the system

The system in Figure 1 is subjected to a white noise, Gaussian, mean zero signal, filtered by the Tajimi-Kanai oscillator, where $\vec{\tau}$ is the influence vector of the filter on the different DOF. The SDF system with n TMDs is transformed in an equivalent system with $(n+2)$ DOFs (one of the main system, the n DOFs added by the dampers, and the DOF associated to the filter.

The main uncertain characteristics of the system are: the mass m_s, damping c_s and stiffness k_s. The vector $\vec{X}(t)$ contains $(n+2)$ values corresponding to the displacements of the main system, of the TMDs and of the filter. $X_s(t)$ consists in the DOF of the main system and $W(t)$ is the white noise input applied to the filter.

Focusing on the MTMD, their main characteristics are described by the diagonal matrices $\boldsymbol{M}$, $\boldsymbol{K}$ ans $\boldsymbol{C}$, reported in the appendix A. No interaction between the TMDs is assumed because they are connected to the main system only and completely disconnected each other. Matrix $\boldsymbol{M_t}$ is defined by a $(n \times 1)$ vector $\vec{\gamma}_t$ that assigns a mass ratio to each TMD, where 1 is the DOF of the main system.

The global matrices (mass, damping, stiffness) of the equivalent $(n+1) \times (n+1)$ system are defined as follow.

$$\boldsymbol{M} = \begin{bmatrix} m_1 & 0 & \dots & \dots & 0 \\ 0 & m_2 & 0 & \dots & \vdots \\ \vdots & & \ddots & & \vdots \\ & & & m_n & 0 \\ 0 & \dots & \dots & 0 & m_s \end{bmatrix}, \tag{1}$$

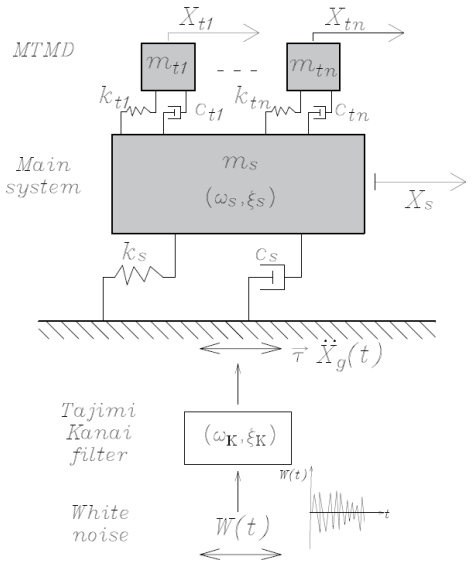


Figure 1: Dynamic scheme of MTMD system for a SDF structure.

$$\boldsymbol{C} = \begin{bmatrix} c_1 & 0 & \dots & \dots & -c_1 \\ 0 & c_2 & 0 & \dots & -c_2 \\ \vdots & & \ddots & & \vdots \\ & & & c_n & -c_n \\ -c_1 & -c_2 & \dots & -c_n & c_s + \sum_{i=1}^{n} c_i \end{bmatrix}, \tag{2}$$

$$\boldsymbol{K} = \begin{bmatrix} k_1 & 0 & \dots & \dots & -k_1 \\ 0 & k_2 & 0 & \dots & -k_2 \\ \vdots & & \ddots & & \vdots \\ & & & k_n & -k_n \\ -k_1 & -k_2 & \dots & -k_n & k_s + \sum_{i=1}^{n} k_i \end{bmatrix}, \tag{3}$$

where the terms of the $\boldsymbol{C}$ matrix in the column $(n+1)$ correspond to the damping transmitted by the main system to the dampers $\vec{C}_{st}$ and the row $(n+1)$ to the damping transmitted by each dampers to the main system $\vec{C}_{ts}$; the last element $(n+1, n+1)$ is the total damping of the main system increased by the contribute of TMDs. The same is valid for the $\boldsymbol{K}$ matrix.

The equation of motions for the main system and the TMDs are, respectively:

$$\begin{cases} m_s \cdot \ddot{X}_s(t) + c_s \cdot \dot{X}_s(t) + \sum_{i=1}^{n} c_i \cdot \dot{\vec{X}}_t(t) + k_s \cdot X_s(t) + \sum_{i=1}^{n} k_i \cdot \vec{X}_t(t) = -m_s \cdot \ddot{X}_g(t) \\ \boldsymbol{M_t} \cdot \ddot{\vec{X}}_t(t) + \boldsymbol{C_t} \cdot \dot{\vec{X}}_t(t) + \vec{C}_{st} \cdot \dot{X}_s(t) + \boldsymbol{K_t} \cdot \vec{X}_t(t) + \vec{K}_{st} \cdot \vec{X}_t(t) = -\vec{\gamma}_t m_s \cdot \ddot{X}_g(t) \end{cases} \tag{4}$$

In Eq. (4), $-\vec{\gamma}_t \cdot \ddot{X}_g(t)$ is the effect of the ground acceleration on the TMDs which is given by the Tajimi Kanai-filter equations [26]:

$$\begin{cases} \ddot{X}_g = -\omega_K^2 \cdot X_K(t) - 2\xi_K \omega_K \cdot \dot{X}_K(t) \\ \ddot{X}_K(t) + 2\xi_K \omega_K \cdot \dot{X}_K(t) + \omega_K^2 \cdot X_K(t) = -W(t) \end{cases} \tag{5}$$

In the state-space representation, the filter is described as follow:

$$\begin{cases} \ddot{X}_g(t) = \vec{a}_K^T \cdot \vec{Y}_K(t) \\ \dot{\vec{Y}}_K(t) = \boldsymbol{D}_K \cdot \vec{Y}_K(t) - \vec{v}_K \cdot W(t) \end{cases} \tag{6}$$

where $W(t)$ is a mean zero, Gaussian, white noise process representing the excitation at the bedrock. The stationary covariance of the white noise excitation is $E[W(t) \cdot W(t-\tau)] = 2\pi S_0 \cdot \delta(t-\tau)$, where $\delta(t-\tau)$ is the Dirac's Delta function and S_0 the power spectrum of the white noise. The other terms in Eq. (6) are:

$$\vec{Y}_K(t) = \begin{bmatrix} \vec{X}_K(t) \\ \dot{\vec{X}}_K(t) \end{bmatrix} \quad \boldsymbol{D}_K = \begin{bmatrix} 0 & 1 \\ -\omega_K^2 & -2\xi_K \omega_K \end{bmatrix}, \quad \vec{v}_K(t) = \begin{bmatrix} 0 \\ 1 \end{bmatrix}, \quad \vec{a}_K = \begin{bmatrix} -\omega_K^2 \\ -2\xi_K \omega_K \end{bmatrix} \tag{7}$$

Grouping the displacements in a vector $\vec{X}(t) = [X_1(t), \ldots, X_n(t), X_s(t)]^T$, the equation of motion (4) can be rewritten in the state-space representation once the state-space vector $\vec{Y}(t)$ is defined:

$$\vec{Y}(t) = [\vec{X}_t(t),\ X_s(t),\ \dot{\vec{X}}_t(t),\ \dot{X}_s(t)]^T \tag{8}$$

The dynamic equilibrium equation becomes:

$$\boldsymbol{A} \cdot \dot{\vec{Y}}(t) + \boldsymbol{B} \cdot \vec{Y}(t) = \vec{p}(t) \tag{9}$$

where:

$$\boldsymbol{A} = \boldsymbol{I}_{2n} = \begin{bmatrix} \boldsymbol{I}_n & \boldsymbol{0} \\ \boldsymbol{0} & \boldsymbol{I}_n \end{bmatrix}, \quad \boldsymbol{B} = \begin{bmatrix} \boldsymbol{0} & \boldsymbol{I}_n \\ -\boldsymbol{M^{-1}K} & -\boldsymbol{M^{-1}C} \end{bmatrix}, \quad \vec{p}(t) = \begin{bmatrix} \vec{0} \\ \boldsymbol{M}^{-1}\vec{F}(t) \end{bmatrix}, \tag{10}$$

$$\boldsymbol{D} = \boldsymbol{A}^{-1}\boldsymbol{B} = \begin{bmatrix} \boldsymbol{0} & \boldsymbol{I}_n \\ -\boldsymbol{M^{-1}K} & -\boldsymbol{M^{-1}C} \end{bmatrix} \tag{11}$$

Once that the system matrices are set, the filtering theory can be used to perform the second order moments analysis of the system. The final state-space equation is:

$$\dot{\vec{Y}}(t) = \bar{\boldsymbol{D}}_{\boldsymbol{N}} \cdot \vec{Y}(t) + \vec{v} \cdot \varphi(t) \cdot W(t) \tag{12}$$

where $\varphi(t) = 1$ for a stationary input and the other terms are the following:

$$\begin{aligned} \vec{Y}(t) &= \begin{bmatrix} \vec{Y}(t) \\ \vec{Y}_K(t) \end{bmatrix}, \quad \bar{\boldsymbol{D}}(t) = \begin{bmatrix} \boldsymbol{D}_N & \boldsymbol{D}_{Nf}(t) \\ \boldsymbol{0} & \boldsymbol{D}_f(t) \end{bmatrix} \\ \vec{v} &= \begin{bmatrix} \vec{0}_{2n} \\ \vec{v}_K \end{bmatrix}, \qquad \boldsymbol{V}_N = \begin{bmatrix} \boldsymbol{0} \\ \boldsymbol{M}^{-1} \end{bmatrix}, \qquad \boldsymbol{D}_{Nf}(t) = \boldsymbol{V}_N \cdot \vec{\tau} \cdot \vec{a}_K^T(t) \end{aligned} \tag{13}$$

The Lyapunov equation is applied to get the covariance matrix of the state-space vector of response, remembering that, for stationary mean zero processes, correlation and covariance coincide [1]. For the case of delta-correlated, stationary, mean zero input, the equation can be written as:

$$\bar{\boldsymbol{D}} \cdot \boldsymbol{R}_{YY}(\tau, \tau) + \boldsymbol{R}_{YY}(\tau, \tau) \cdot \bar{\boldsymbol{D}}^T = 2\pi \boldsymbol{A}^{-1} S_0(\tau)\ (\boldsymbol{A}^{-1})^T \tag{14}$$

Defining $\boldsymbol{P} = 2\pi \boldsymbol{A}^{-1} S_0(t)\ (\boldsymbol{A}^{-1})^T$, Eq. (14) becomes:

$$\boldsymbol{D} \cdot \boldsymbol{R}_{YY}(\tau, \tau) + \boldsymbol{R}_{YY}(\tau, \tau) \cdot \boldsymbol{D}^T = \boldsymbol{P} \tag{15}$$

where $\tau = t_2 - t_1$, and $\boldsymbol{R}_{YY}$ is the stationary covariance (remembering that the mean of the response is zero). Eq. (15) can be solved by a Shur decomposition [27], and the covariance of the acceleration can be obtained from the state-space equation (9):

$$\dot{\vec{Y}}(t) = \boldsymbol{A}^{-1}\boldsymbol{B} \cdot \vec{Y}(t) + \boldsymbol{A}^{-1}\vec{p}(t) = \boldsymbol{D} \cdot \vec{Y}(t) + \vec{p}(t) \tag{16}$$

that in expanded form becomes:

$$\vec{Y}(t) = \begin{bmatrix} \vec{X}(t) \\ \dot{\vec{X}}(t) \end{bmatrix} = \begin{bmatrix} \mathbf{0} & \boldsymbol{I}_n \\ -\boldsymbol{M^{-1}K} & -\boldsymbol{M^{-1}C} \end{bmatrix} \cdot \begin{bmatrix} \vec{X}(t) \\ \dot{\vec{X}}(t) \end{bmatrix} + \begin{bmatrix} \vec{0} \\ \boldsymbol{M}^{-1}\vec{F}(t) \end{bmatrix} \tag{17}$$

where the applied force is the ground acceleration output of the filter, $\boldsymbol{M}^{-1}\vec{F}(t) = -\ddot{\vec{X}}_g$. Considering the second term of the equation, and expanding it:

$$\ddot{\vec{X}} = \begin{bmatrix} -\boldsymbol{M^{-1}K} & -\boldsymbol{M^{-1}C} \end{bmatrix} \cdot \begin{bmatrix} \vec{X}(t) \\ \dot{\vec{X}}(t) \end{bmatrix} - \ddot{\vec{X}}_g \tag{18}$$

The inertial forces induced on the structure depend on the absolute acceleration $\ddot{\vec{X}}_{tot} = \ddot{\vec{X}} + \ddot{\vec{X}}_g$. Therefore, the total acceleration can be computed as:

$$\ddot{\vec{X}}_{tot} = \begin{bmatrix} -\boldsymbol{M^{-1}K} & -\boldsymbol{M^{-1}C} \end{bmatrix} \cdot \begin{bmatrix} \vec{X}(t) \\ \dot{\vec{X}}(t) \end{bmatrix} = \boldsymbol{V} \cdot \vec{Y} \tag{19}$$

Applying the linear operator mean to the product $(\ddot{\vec{X}}_{tot} \cdot \ddot{\vec{X}}_{tot}^T)$ the covariance matrix of the absolute acceleration can be computed as:

$$E[\ddot{\vec{X}}_{tot} \cdot \ddot{\vec{X}}_{tot}^T] = \boldsymbol{R}_{\ddot{X}_{tot}\ddot{X}_{tot}} = \boldsymbol{V} \cdot \begin{bmatrix} \boldsymbol{R}_{XX} \\ \boldsymbol{R}_{\dot{X}\dot{X}} \end{bmatrix} \cdot \boldsymbol{V}^T \tag{20}$$

The problem of optimization in the random vibration field was first formulated by Nigam [10]:

- Find the *design vector* $\vec{d} = (\vec{\omega}_t, \vec{\xi}_t) \in \Omega_d$ (where Ω_d is the admissible space of the design parameters);
- that minimizes the *objective function* bi-dimensional vector $\vec{OF} = [\mu_{OF}, \sigma_{OF}]$, containing the mean and standard deviation (or sensitivity) of the ratio between protected and unprotected response;
- given the *constraints* $g_i(\vec{d}) \leq 0$ for $i = 1,\ 2, \ldots,\ k$; where k is the number of constraints.

The ratio assumed as OF takes the name of *index of vibration protection effectiveness*. A value smaller than one indicates that the protection is effective,

while a value bigger than the unity means a worsening of the performance, as small is the index as big is the improvement. A minimum of the index corresponds to an optimum of the system performance in terms of displacements (i.e., the structure damaging):

$$OF_{displ} = \frac{\sigma_{XX}}{\sigma_{XX,0}} \tag{21}$$

or absolute accelerations (i.e., the internal comfort):

$$OF_{acc} = \frac{\sigma_{\ddot{X}_{tot}\ddot{X}_{tot}}}{\sigma_{\ddot{X}_{tot}\ddot{X}_{tot},0}} \tag{22}$$

3. Direct perturbation method and uncertain

To obtain the sensitivity of the system, that is, the standard deviation from the design value of the response, the direct perturbation method is applied. The uncertain parameters assumed are: the natural frequency of the main system ω_s, the damping ratio of the main system ξ_s, the frequency of the Tajimi-Kanai filter ω_K and the damping ratio of the Tajimi-Kanai filter ξ_K, the mass ratio of the tuned mass dampers γ_t. They are all collected in the vector of uncertain parameters $\vec{d} = [\omega_s, \xi_s, \omega_k, \xi_k, \gamma_t]$. The dependence between these parameters is small, but in general not nil. However, the assumption of statistically independent parameters is adopted. Once the derivatives respect to these parameters are set, the sensitivity of the objective function is determined assuming a linear approximation:

$$E[Q_{lin}] = Q_0 = \mu_Q \tag{23}$$

$$Var[Q_{lin}] = \sum_{l=1}^{R} \beta_{lk}^2 \cdot \sigma_{Rl}^2 \tag{24}$$

where the mean value is assumed coincident with the target design, β_{lk} are the sensitivity coefficients and σ_{Rl}^2 the variance of each design parameter. The use of the linear perturbation method allows to work still in the field of linearity and, after performing the previous analysis, to obtain again a mean zero stationary Gaussian output, given a mean zero stationary Gaussian input.

The derivatives of the objective functions in Eq. (21) and Eq. (22) are, respectively:

$$(OF_{displ})_{d_i} = \frac{-(\sigma_{XX})_{d_i} \cdot \sigma_{XX,0} + (\sigma_{XX,0})_{d_i} \cdot \sigma_{XX}}{\sigma^2_{XX,0}} \tag{25}$$

$$(OF_{acc})_{d_i} = \frac{-(\sigma_{\ddot{X}_{tot}\ddot{X}_{tot}})_{d_i} \cdot \sigma_{\ddot{X}_{tot}\ddot{X}_{tot},0} + (\sigma_{\ddot{X}_{tot}\ddot{X}_{tot},0})_{d_i} \cdot \sigma_{\ddot{X}_{tot}\ddot{X}_{tot}}}{\sigma^2_{\ddot{X}_{tot}\ddot{X}_{tot},0}} \tag{26}$$

The standard deviation in the previous equations is obtained from the variance as:

$$\sigma_{XX} = \sqrt{\sigma^2_{XX}} \tag{27}$$

Consequently, the derivative is:

$$(\sigma_{XX})_{di} = -\frac{1}{2}\frac{(\sigma^2_{XX})_{di}}{\sqrt{\sigma^2_{XX}}} \tag{28}$$

and the same for $(\sigma_{\dot{X}\dot{X}})_{di}$ and $(\sigma_{\ddot{X}_{tot}\ddot{X}_{tot}})_{di}$. For what concerns the variance of acceleration, it depends linearly from the other variances, as stated in Eq. (20), and its derivative is:

$$\boldsymbol{R}_{\ddot{X}_{tot}\ddot{X}_{tot}} = 2 \cdot (\boldsymbol{V})_{d_i} \cdot \begin{bmatrix} \boldsymbol{R}_{XX} \\ \boldsymbol{R}_{\dot{X}\dot{X}} \end{bmatrix} \cdot \boldsymbol{V}^T + \boldsymbol{V} \cdot \begin{bmatrix} \boldsymbol{R}_{XX} \\ \boldsymbol{R}_{\dot{X}\dot{X}} \end{bmatrix}_{d_i} \cdot \boldsymbol{V}^T \tag{29}$$

The derivative of the Lyapunov equation is calculated considering the linearity of the operator, grouping all the linear operations in lyap($\bullet$). In this way, it can be written as:

$$\boldsymbol{R}(\vec{d}) = \text{lyap}(\vec{d}) \tag{30}$$

and its derivative respect to the i^{th} uncertain parameter is:

$$\left(\boldsymbol{R}(\vec{d})\right)_{d_i} = \left(\frac{\partial[R(\vec{d})]}{\partial d_i}\right)_{\vec{d}=\vec{\mu}_d} = \left(\frac{\partial\left[\text{lyap}(\vec{d})\right]}{\partial d_i}\right)_{\vec{d}=\vec{\mu}_d} \tag{31}$$

Applying this to Eq. (15) gives:

$$\boldsymbol{D}\cdot(\boldsymbol{R}_{YY})_{d_i} + (\boldsymbol{R}_{YY})_{d_i}\cdot\boldsymbol{D}^T + \boldsymbol{H}_i = \boldsymbol{0}, \qquad \boldsymbol{H}_i = (\boldsymbol{D})_{d_i}\cdot\boldsymbol{R}_{YY} + \boldsymbol{R}_{YY}\cdot(\boldsymbol{D}^T)_{d_i} + (\boldsymbol{P})_{d_i} \tag{32}$$

$(\boldsymbol{P})_{d_i} = \mathbf{0}$ results because of its independence from the uncertain parameters. Applying the operator lyap($\bullet$) to Eq. (32) gives the derivative of the variance $(\boldsymbol{R}_{YY})_{d_i}$ respect to each uncertain parameter. The derivatives of $(\boldsymbol{D})_{d_i}$ with respect to each element of the vector $\vec{d}$ have been calculated both for the protected and unprotected case. The detailed results are reported in the appendix A.

Once the sensitivity coefficient β is determined, the mean and the variance can be computed by Eq. (23) and (24). From the variance, the standard deviation is derived as its square root, and a bi-dimensional robust optimization vector is set up. It contains the mean and standard deviation of the index of protection effectiveness:

$$\vec{OF} = [\mu_{OF}, \sigma_{OF}] \tag{33}$$

4. Optimization algorithm

The first step in the optimization is checking if the design domain is convex or differently, in order to adopt the best algorithm for the analysis. Either for the mean value that for the standard deviation, the design space is not convex due to the peaks and valleys that characterize the response with more TMDs. Therefore, the optimization cannot be performed properly by an ordinary gradient analysis, and an heuristic method has to be applied. In this paper, a genetic algorithm with not articulated preferences is used. The main advantage of this approach is to avoid influences on the Pareto front shape and possible biases induced by wrong evaluations done by the designer. The design is performed by fixing uniform damping ratio and varying tuning ratios between the dampers, therefore the problem size, i.e. the number of parameters to be optimized, is $n_{tmd} + 1$.

In the MOOP the concept of optimum is slightly different from the single-objective optimization (SOP). In SOP the feasible set is completely ordered

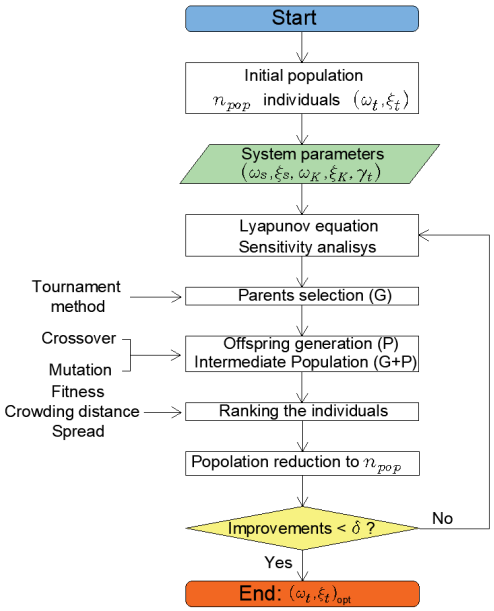


Figure 2: Genetic Algorithm flow chart.

according to the single value of the objective function f and can be easily compared in order to get the searched optimum. In MOOP, instead, the solutions can be only partially according to ranks of dominance and more possible optimum conditions have to be considered [28].

The adopted algorithm is an unbounded, controlled, elitist genetic algorithm, variant of the NSGA-II method [29]. An elitist GA always favors individuals with better fitness value (rank), but also favors individuals that can help to increase the diversity of the population even if they have a lower fitness value. A scheme of the algorithm is reported in a flow chart in Figure 2.

The individuals are ordered in *ranks* according to their dominance position and the algorithm tracks the *crowding distance*: a measure of the closeness of an individual to its nearest neighbors of the same rank in the objective function space. The distance of individuals at the extreme positions are set to infinity. For the remaining ones, the distance is taken as a sum over the dimensions

of the normalized absolute distances between the individual's sorted neighbors. Mathematically, for a problem of dimension m and sorted, scaled individual i, the distance $d(i)$ is:

$$d(i) = \sum_{i=1}^{m} \big[x(m, i+1) - x(m, i-1)\big] \tag{34}$$

The algorithm sorts each dimension separately, so the neighbors are intended for each dimension. Individuals of the same rank with a higher distance do have more chances of selection (because the distance grants the population diversity). The crowding distance is also one factor in the calculation of the spread, which is part of a stopping criterion, and it is used as a tie-breaker in tournament selection when two selected individuals have the same rank.

The *spread* is a measure of the movement of the Pareto set. To calculate it, the algorithm first evaluates σ, the standard deviation of the crowding distance of the points that are on the Pareto front. The algorithm then evaluates μ, the sum over the k^{th} objective function indices of the norm of the difference between the current minimum value Pareto point for that index and the value in the previous iteration. The spread is then:

$$\text{spread} = \frac{\mu + \sigma}{\mu + k \cdot \sigma} \tag{35}$$

The value is small when the extreme objective function values do not change much between iterations (that is, μ is small) and when the points on the Pareto front are spread evenly (that is, σ is small).

According to the fitness, crowding distance and spread, the population is ranked and the best individuals are compared with the previous generation for the algorithm stopping criteria, iterating towards the final optimum.

5. Obtained results

This section is focused on the results from benchmark applications. Details are reported in appendix-B in terms of complete tabular results, while the graphical outcomes are showed and discussed within this section.

Table 1: Initial data for the deterministic optimization with varying ψ

ω_s (rad/s)	ξ_s $(-)$	γ_t $(-)$	ω_K (rad/s)	ξ_K $(-)$	S_0 (cm^2/s^3)
[2.5, 20.0]	0.02	0.05	12.5	0.4	1000

5.1. Deterministic analysis

A deterministic analysis is performed for both displacements and absolute accelerations, considering different frequencies of the main system. As first approach, for equal optimal damping of the TMDs and fixed filter frequency ω_K, a varying frequency ω_s is investigated. As stated by different authors ([30] and [31]), fixing equal damping ratio does not leads to particularly different results from a free parameters analysis. Indeed, for free parameters the optimum TMD tents to assume a spread tuning ratio at a fixed value of damping ratio. Moreover, the use of a uniform MTMD results in a robustness improvement because the loss of one damper does not compromise significantly the performance ([32] and [24]). Defined the *frequency ratio* ψ between main system and filter, remembering the definition of tuning ratio ρ:

$$\psi = \frac{\omega_s}{\omega_K}, \qquad \rho = \frac{\omega_t}{\omega_s} \tag{36}$$

and assumed medium soil conditions ($\omega_K = 12.5$ rad/s, $\xi_K = 0.4$), the optimization is performed. The adopted data are reported in Table 1. The analysis has been performed for a number of dampers varying from 1 to 10 either for absolute accelerations that for displacements.

Referring to the displacements, Figure 3a reports the frequency values for different number of dampers and frequency ratio ψ, while Figure 3b reports the OF values. Accordingly with Marano et al. [33], for frequency ratios $\psi > 1$, the frequencies of the optimal TMDs increase, while they decrease for $\psi < 1$ (except for low values of ψ where the tuning becomes difficult). For what concerns the absolute accelerations, the frequencies values for different number of dampers and frequency ratio ψ are reported in Figure 4a, while the OF values can be found in Figure 4b. The numerical values assumed by the OFs are also tabled

in appendix B. As expected, when the frequency ratio is near to the resonance, i.e $\psi \approx 1$, the performances improve. Conversely, the performances in terms of displacements worsen if the number of dampers is increased, leading to a failure of the protection system when a certain number is overcome. The absolute acceleration performances instead benefit from the increase of the number of dampers except when the frequency ratio assumes low values ($\psi \leq 0.4$), that is, the main mode of the system is characterized by a low frequency and the structure is slender.

In general, both the acceleration and displacements performances are worsened in slender structures by the use of MTMDs due to a difficult in properly tuning the system. This may be explained by the shape of the Power Spectral Density functions (PSD) of the system for the Tajimi-Kanai spectrum defined as [26]:

$$S_{\ddot{X}_g} = \frac{(\omega_K^4 + \xi_K^2 \omega_K^2 \omega^2) S_0}{(\omega_K^2 - \omega^2)^2 + 4\xi_K^2 \omega_K^2 \omega^2} \equiv S_{TK}(\omega) \tag{37}$$

where S_0 is the power spectrum of the white noise process and the lowercase K indicates the properties of the ground, while the others are the properties of the structure. The difficult tuning in terms of displacements at the increasing of dampers can be observed if the transfer function $H_X(\omega)$ is analyzed. The variance of displacements has a quadratic relation with the PSD:

$$\sigma_X^2 = \int_{-\infty}^{+\infty} |H_X(\omega)|^2 \cdot S_{\ddot{X}_g}(\omega)\ d\omega = \int_0^{+\infty} |H_X(\omega)|^2 \cdot G_{\ddot{X}_g}(\omega)\ d\omega \tag{38}$$

For a SDF system the harmonic transfer matrix takes the form:

$$H_X(\omega) = [k - \omega^2 m + i\omega c]^{-1} = \frac{1}{(\omega_s^2 + 2i\xi_s\omega - \omega^2)} \tag{39}$$

In the single degree of freedom case the relation between displacements and acceleration harmonic transfer matrices is given by $H_{\ddot{X}}(\omega) = \omega^2 \cdot H_X(\omega)$, while for MDF systems is necessary a modal decomposition, with similar results. For the SDF system it becomes:

$$H_{\ddot{X}}(\omega) = \frac{\omega^2}{(\omega_s^2 + 2i\xi_s\omega - \omega^2)} \tag{40}$$

The associated variance is:

$$\sigma^2_{\ddot{X}} = \int_{-\infty}^{+\infty} |\omega^2 \cdot H_{\ddot{X}}(\omega)|^2 S_{\ddot{X}_g}(\omega)\ d\omega = \int_{0}^{+\infty} |\omega^2 \cdot H_{\ddot{X}}(\omega)|^2 G_{\ddot{X}_g}(\omega)\ d\omega \quad (41)$$

The PSD of the Tajimi-Kanai spectrum, $S_{\ddot{X}_g}$ is reported in Figure 5. The correspondent PSD of acceleration, $S_{\ddot{X}\ddot{X}}$ is plotted for the system parameters in Figure 6. The Tajimi-Kanai PSD of displacements diverges for values of $\omega \to 0$, this is not a problem in a time analysis but becomes so if the spectrum are used; for sake of clarity, a correspondent Clough-Penzien spectrum is given in Figure 7 with the associated $S_{XX}(\omega)$ of displacements in Figure 8. The filter is a modified version of the Tajimi-Kanai one based on two consequential filters with parameters ω_P, ξ_P and ω_K, ξ_K [34] :

$$S_{\ddot{X}_g} = S_{TK}(\omega) \cdot \frac{\omega^4}{(\omega_P^2 - \omega^2) + 4\xi_P^2\omega_P^2\omega^2} \equiv S_{CP}(\omega) \quad (42)$$

where the parameters of the filters have to be determined experimentally by using registered acceleration histories. Another limits of the Tajimi-Kanai spectrum is also the fact that, for $\omega \to 0$, $S_{\ddot{X}\ddot{X}}$ does not go to zero too. However, for intermediate frequencies, the spectrum can be used without problems and gives an immediate picture of the resonance effects.

The PSD of acceleration shows a wider band of magnified frequencies compared to the PSD of displacements. As the number of TMDs increases, the tuning ratio of part of them decreases, while only some are tuned to higher values (see Figure 3a and Figure 4a); overall, the bandwidth increases. The TMDs cannot actually be tuned to the same frequency of a single TMD because the system increases of degrees of freedom and this modifies the behavior of the structure, with more peaks and valleys in the response due to the different modal shapes. The very narrow band nature of the PSD of displacements makes difficult a proper tuning of a MTMD with an increasing bandwidth and the performance worsen because there are amplifications of the PSD (of which the subtended area corresponds to the variance of the process). In the case of acceleration, the more broad band nature of the PSD makes the MTMD better perform as the bandwidth increases. For very slender structures, ($\psi \to 0$), the

Table 2: Deterministic optimization initial data for the analyzed case

ω_s (rad/s)	ξ_s $(-)$	γ_t $(-)$	ω_K (rad/s)	ξ_K $(-)$	S_0 (cm^2/s^3)
13.96	0.02	0.05	18.62	0.4	1000

PSD of acceleration flattens, while the PSD of displacements shows a very sharp peak; both the phenomena are a reason for the worsening of performance as the number of dampers increases: a sharp peak is difficult to be covered without undesired amplification in its neighborhood, while a flat curve is difficult to be managed by a MTMD with more peaks and valleys that may up-cross it. Actually, the PSD integration is not the adopted approach for the analysis but yet it can explain the physical aspects behind the results. As demonstrated by Marano et al. [35], this behavior is also influenced by the nature of the soil, in fact, soft soils imply wider displacements while stiff soils involve bigger accelerations.

5.2. Deterministic sample analysis

In the light of previous considerations, a sample stiff structure on a stiff soil is analyzed in order to determine the best number of dampers to control displacement and acceleration. The data for the analysis are reported in Table 2.

Figure 9 shows the parameters space values. Increasing the number of TMDs only some dampers are tuned to higher frequencies, while the others assume a narrow spacing at lower frequencies. Being the frequency ratio $\psi < 1$, the tuning ratio $\rho < 1$, similarly to what demonstrated by Marano et al. [33] for the single TMD .

Figure 10 shows the parameters space values. As for the displacements, increasing the number of TMDs, they assume a narrow spacing, lower frequencies and a wider bandwidth. Being the ratio $\psi < 1$, the tuning ratio $\rho < 1$ too as for the displacements.

In Figure 11 both the objective functions for varying number of dampers are reported. Increasing the number of dampers worsen the performances in

terms of displacements, because only part of them are properly tuned, while the others work as damping devices. Instead, for the acceleration, the same leads to better performances.

Overall, for stiff structures the choice of the number of dampers is not immediate because the acceleration and displacement diverge in the optimal choice. If, considering displacements, increasing the number of dampers is problematic for the previously stated reasons, the absolute acceleration suffers only for lower system frequency. Consequently, a trade-off between the two parameters has to be adopted in the design.

5.3. Robust optimization

As anticipated, the aleatory nature of the system may induce dangerous deviations from the design target that, for the robustness purpose, have to be quantified and contained. Therefore, a robust optimization of both displacements and absolute acceleration is performed in this section for the same data of Table 2 and the coefficient of variation of the uncertain parameters, $\eta = \sigma/\mu$, in Table 3. The design parameters are the same already adopted, ω_t and ξ_t. The size of the problem is $(n_{tmd} + 1)$, the Pareto fronts are considered from 1 to 10 dampers and some values are extracted from the curves for the aim of comparison. On the same graphs, the results obtained by adopting the optimal deterministic parameters applied in presence of uncertainties are plotted. As expected, the points are at the extreme of the Pareto fronts, maximizing only the effectiveness with the worst values in terms of robustness. The standard deviation assumes significant values (around $0 \div 10\%$ for displacements), considering a value of $\pm 3\sigma$ (Gaussian distribution) to cover almost all the values of the distribution.

5.3.1. Displacements robust control

Figure 12 shows the parameters space values for the case, and Figure 13 the associated Pareto front.

Table 3: Coeff. of variation, $\eta = \sigma/\mu$, of the uncertain parameters in the analyzed case

ω_s $(-)$	ξ_s $(-)$	γ_t $(-)$	ω_K $(-)$	ξ_K $(-)$
0.15	0.20	0.05	0.15	0.10

In the displacements control, the curves are quite flat, showing that every solution has a similar level of robustness. For instance, for 3 TMDs and fixed damping ratio, a decrease of 20% in the mean value implies just an increase of 2% in sensitivity.

For the single TMD, higher damping ratios and lower tuning ratios correspond to more robust but less effective solutions. Increasing the number of dampers, the bandwidth, and consequently the robustness, increase, while the effectiveness worsen. In contrast, increasing the damping ratios improves robustness, while worsen the effectiveness. As for the deterministic case, only part of the TMDs is tuned to higher frequencies, while the others remain closely spaced at lower tuning ratios. This means a lower tuned mass and worse performance of the MTMD compared to the TMD. After a certain number of dampers the tuning becomes difficult, and both effectiveness and robustness worsen. In Figure 19, the fronts are reported for a number from 1 to 5 dampers, to have better comparable curves. The correspondent space parameters values are reported in Figure 18. The same points are also tabled in appendix B.

5.3.2. Accelerations robust control

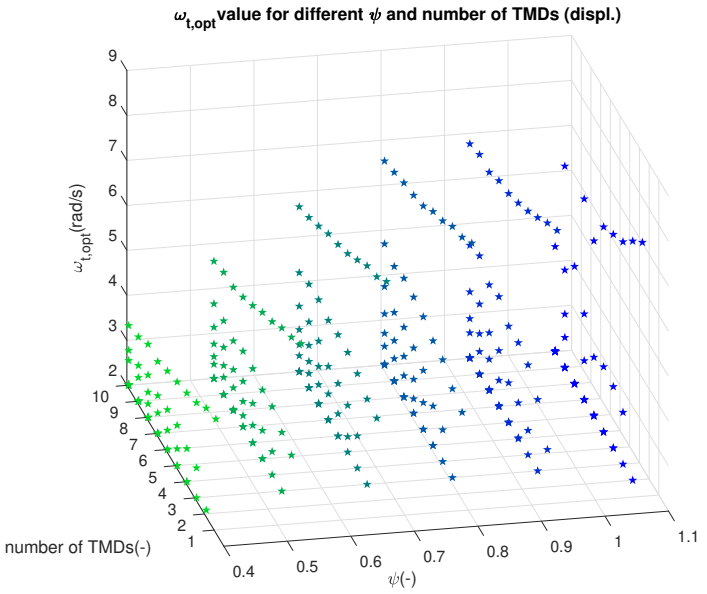
Figure 16 shows the parameters space values for the Pareto fronts, and Figure 17 together with the values from the optimal deterministic design parameters.

In accelerations control, the curves are very skew, showing that a small gain in terms of effectiveness is paid expensively in terms of robustness. For instance, for 3 TMDs and fixed damping, a decrease of 10% in the mean value implies an increase of 2% of sensitivity. However, for the analyzed case, the performances, either in terms of mean and standard deviation, are better than displacements. For instance, considering a number between 1 and 5 TMDs, the reduction of

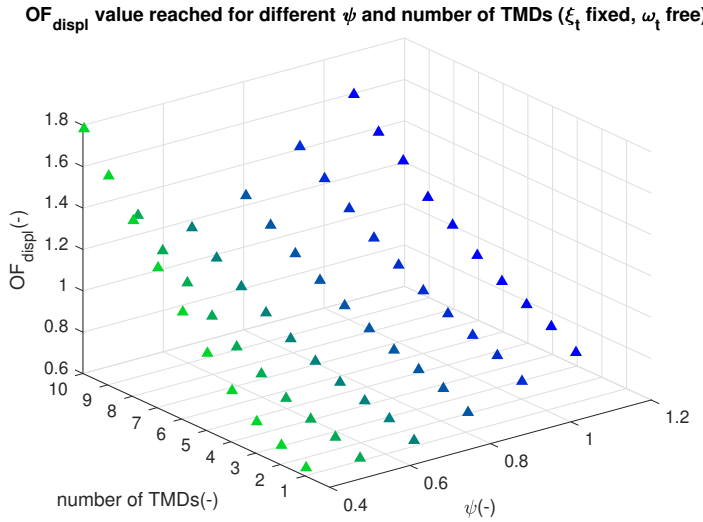
acceleration arrives until the 65% compared to only a 35% in terms of displacements, while the sensitivity is kept between the 1% and 3%, compared to a 1% to 10 % for displacements. The use of a single TMD results in a two fragments front, where the choice is between high performances with low robustness or vice versa. Increasing the number of TMDs leads to more compact curves, resolving this problem. For the single TMD, higher damping ratios and lower tuning ratios correspond to more robust but less effective solutions. Increasing the number of dampers, the uniformly distributed bandwidth and small variations in damping lead to great gains in robustness, showing that MTMD better performs with respect to the single TMD. In fact, all the TMDs are tuned to higher frequencies and remain closely spaced. Overall, increasing the number of TMDs aims to attain a higher level of robustness and performances.

As for the deterministic case, the best performances in terms of acceleration or displacement are not attained in the same direction. Increasing the number of dampers always leads to more robust solutions, but after a certain number the performance of displacements are no more acceptable due to the impossibility of a proper tuning.

Figure 15 reports the Pareto fronts from 1 to 5 dampers to have better comparable curves. The correspondent space parameters values are reported in Figure 14 with some marked reference points. They are also tabled in appendix B.

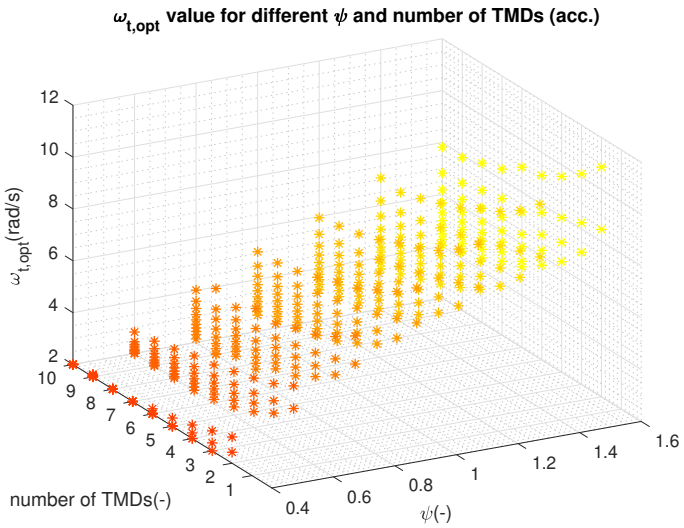


(a) $\omega_{t,opt}$ dipl. deterministic optimal values for varying ψ and number of TMDs.

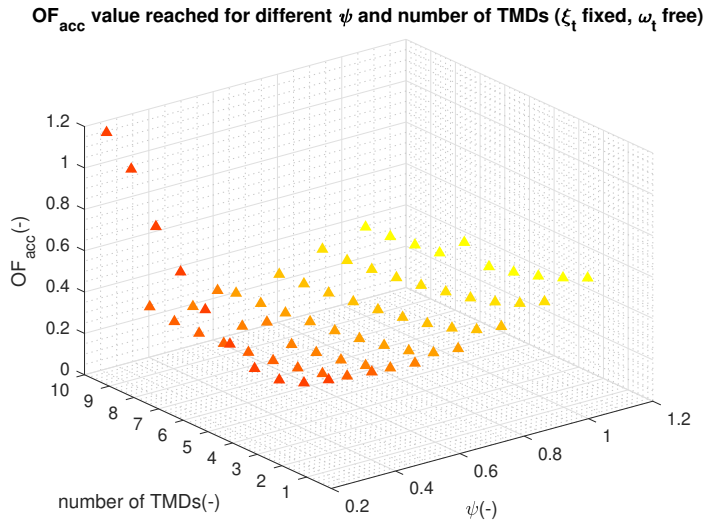


(b) OF dipl. deterministic optimal values for varying ψ and number of TMDs

Figure 3: Optimal parameters and OF_{displ} for varying frequency ratio ψ and number of TMDs



(a) $\omega_{t,opt}$ acc. deterministic optimal values for varying ψ and number of TMDs.



(b) OF acc. deterministic optimal values for varying ψ and number of TMDs

Figure 4: Optimal parameters and OF_{acc} for varying frequency ratio ψ and number of TMDs

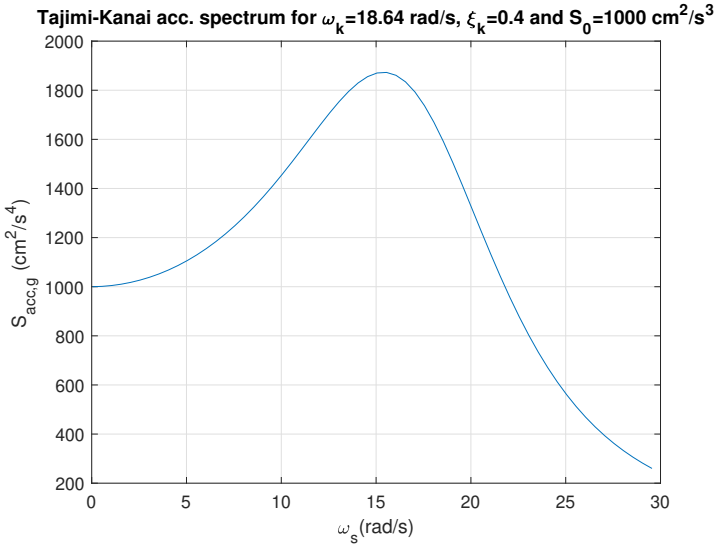


Figure 5: Tajimi-Kanai PSD for $\omega_K = 18.64\ rad/s$, $\xi_K = 0.4$ and $S_0 = 1000\ cm^2/s^3$.

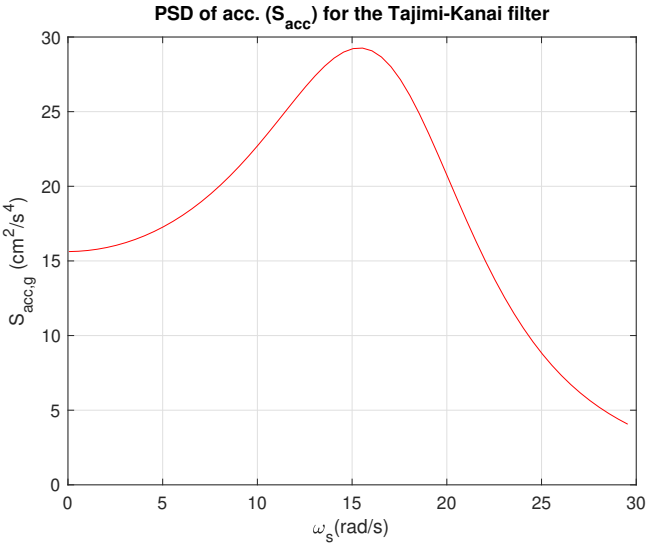


Figure 6: PSD of acc. $S_{\ddot{X}\ddot{X}}$, for the Tajimi-Kanai spectrum in Figure 5, $\omega_s = 13.96\ rad/s$ and $\xi_s = 0.05$.

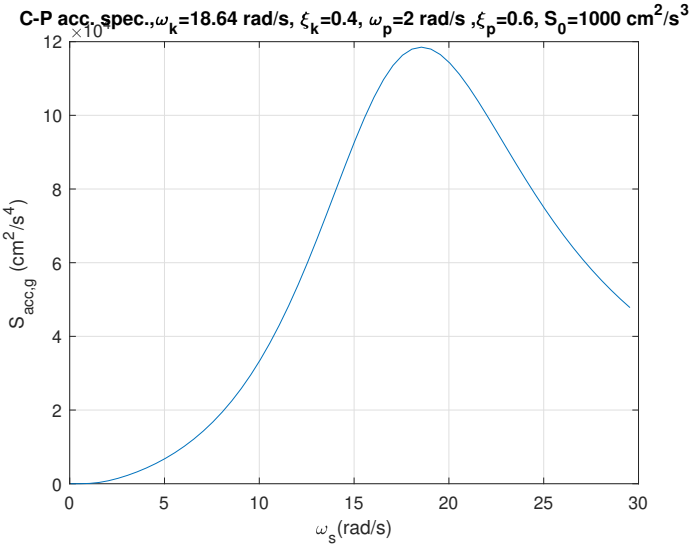


Figure 7: Clough-Penzien PSD for $\omega_K = 18.64\ rad/s$, $\xi_K = 0.4$, $\omega_P = 2.0\ rad/s$, $\xi_P = 0.6$ and $S_0 = 1000\ cm^2/s^3$.

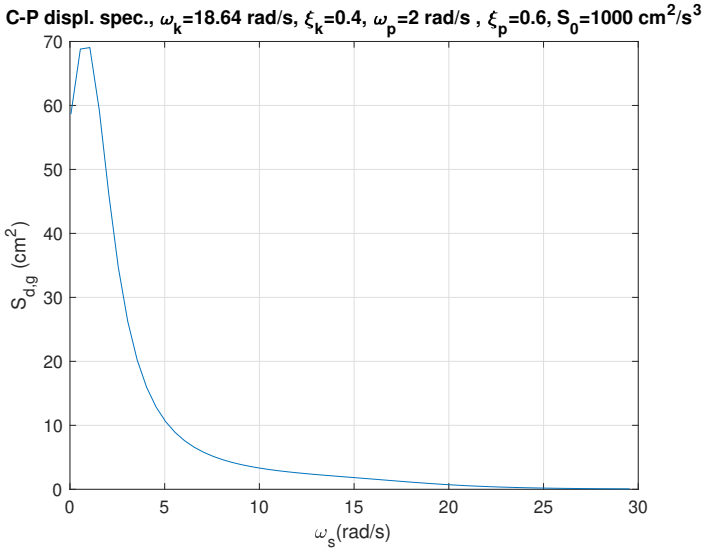


Figure 8: PSD of displ., S_{XX}, for the Clough-Penzien spectrum in Figure 7, $\omega_s = 13.96\ rad/s$ and $\xi_s = 0.05$.

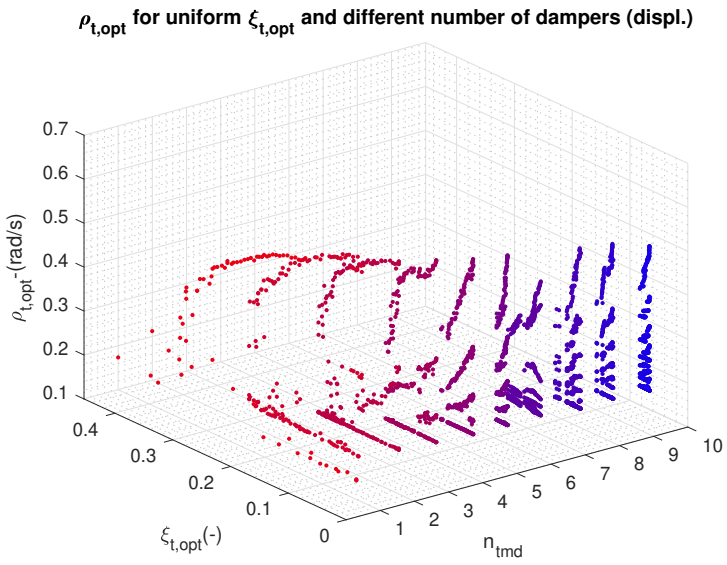


Figure 9: Deterministic optimal tuning ratios for uniform damping ratio (displ.).

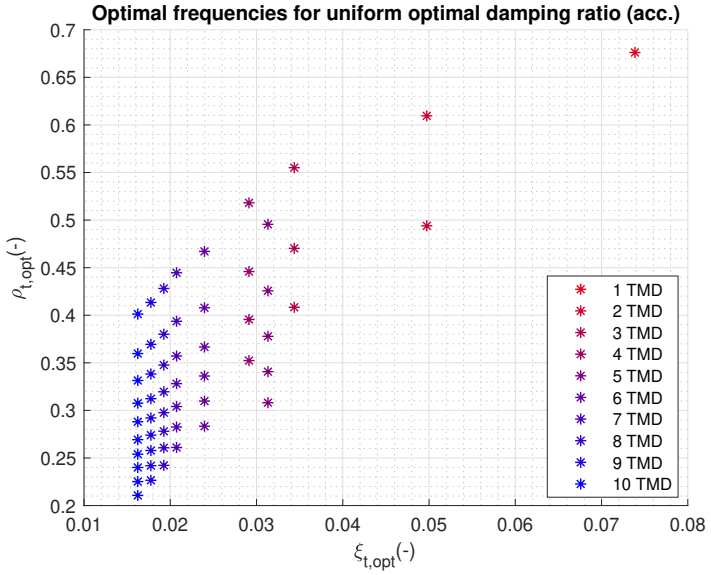


Figure 10: Deterministic optimal tuning ratios for uniform damping ratio (acc.).

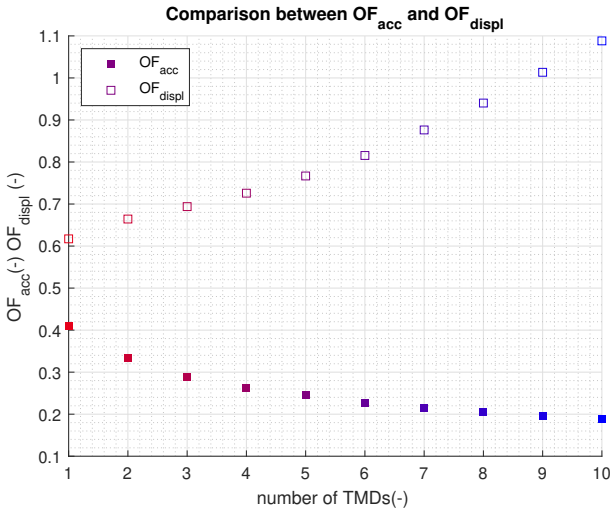


Figure 11: OF_{displ} and OF_{acc} deterministic analysis comparison for fixed damping ratio.

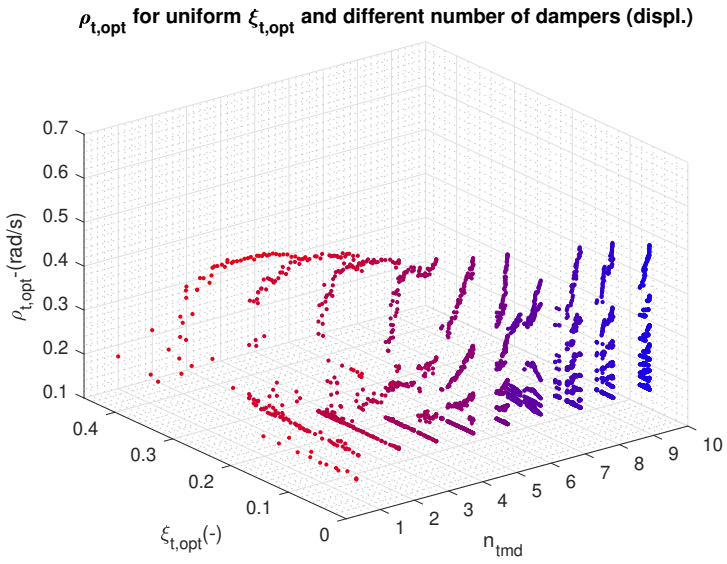


Figure 12: Robust optimal frequencies for uniform damping ratio (displ.).

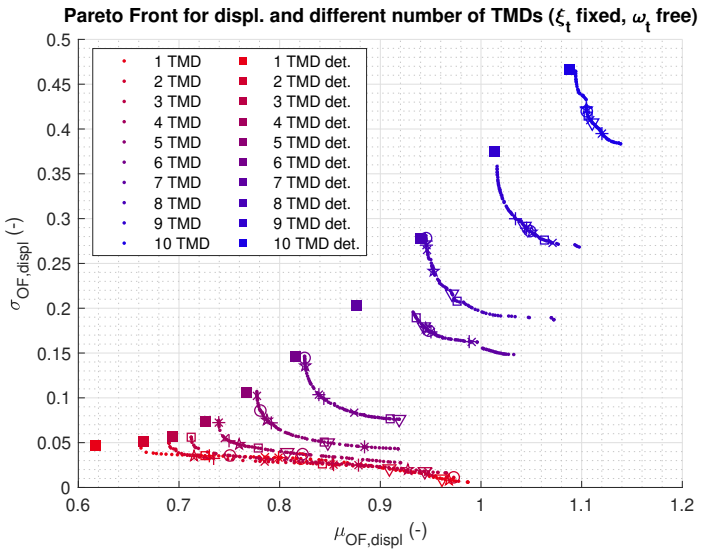


Figure 13: Pareto front for uniform damping ratio (displ.).

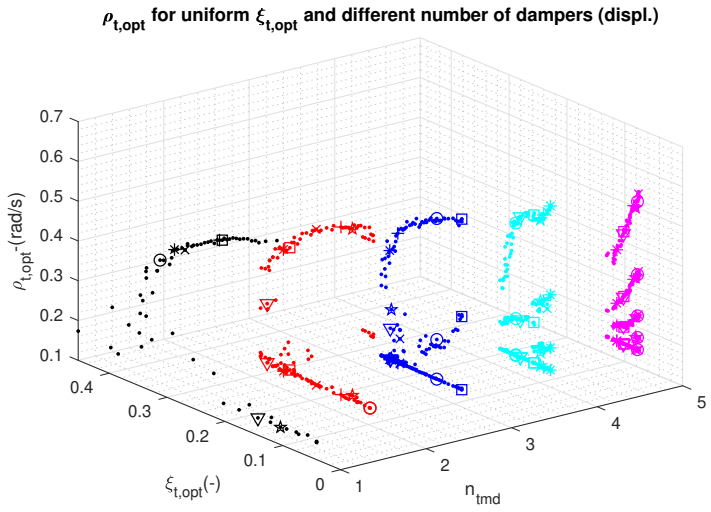


Figure 14: Reduced robust optimal frequencies for uniform damping ratio (displ.)

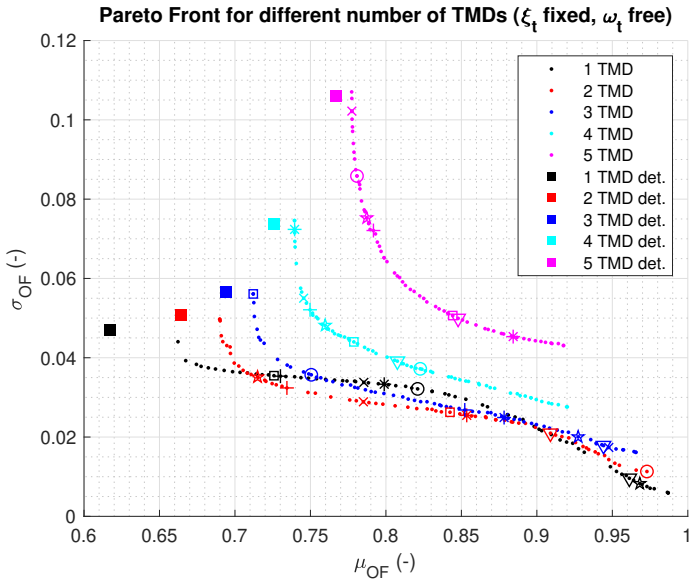


Figure 15: Reduced Pareto fronts for uniform damping ratio (displ.)

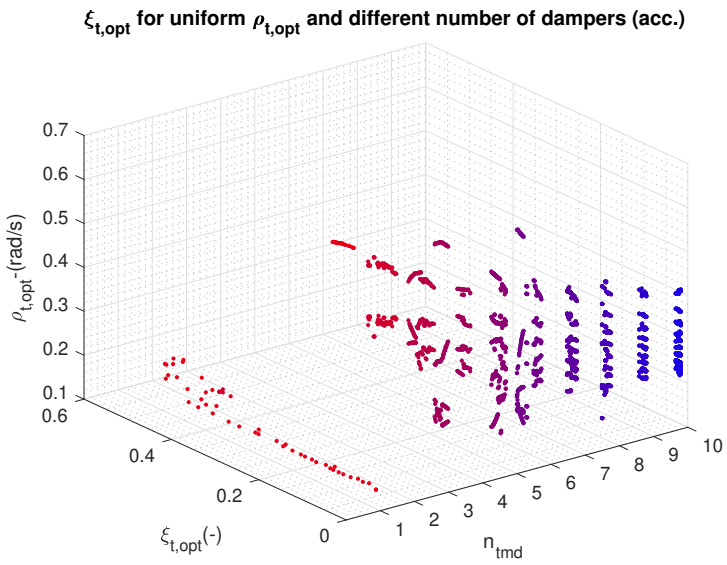


Figure 16: Robust optimal frequencies for uniform damping ratio (acc.)

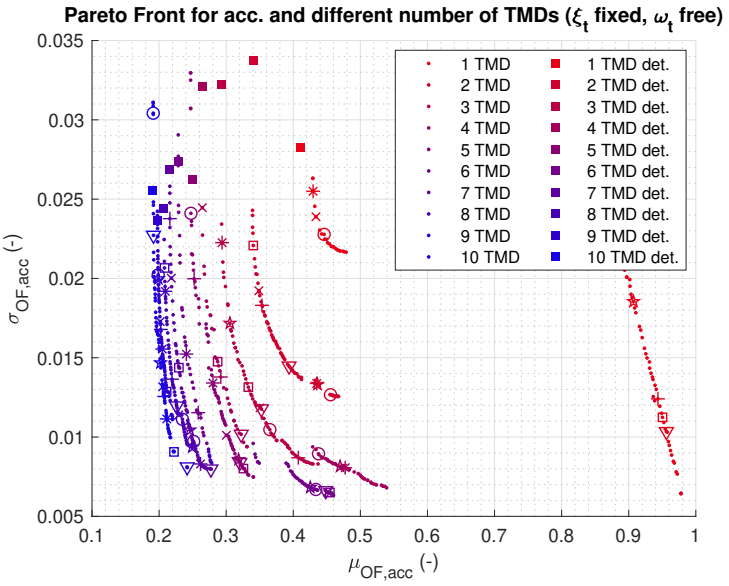


Figure 17: Pareto fronts for uniform damping ratio (acc.)

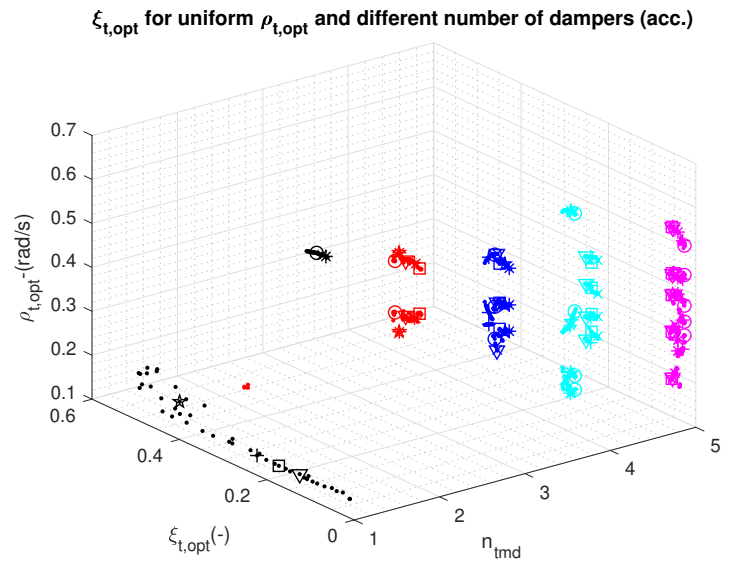


Figure 18: Reduced robust optimal frequencies for uniform damping ratio (acc.)

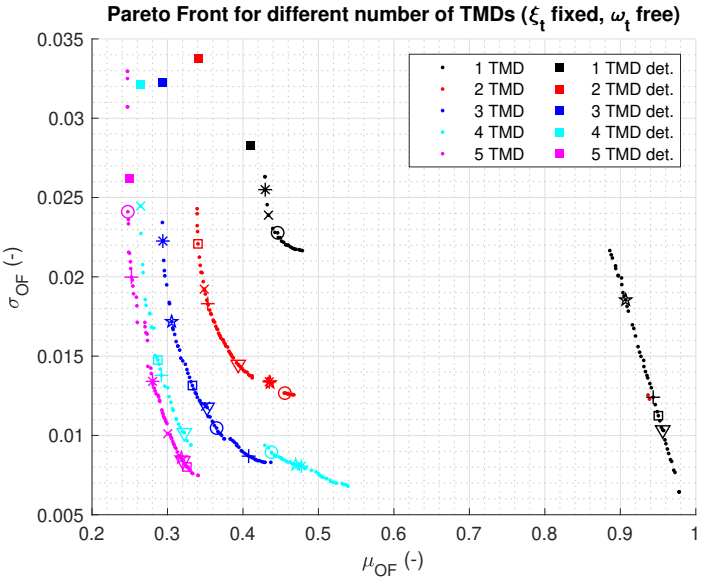


Figure 19: Reduced Pareto fronts for uniform damping ratio (acc.)

6. Conclusions

A robust optimal design criterion for a MTMD device in case of random vibrations is proposed. Robustness is obtained finding a solution that considers not only the absolute performance but also its sensitivity to system parameters variation due to uncertainties. The dynamic input is represented by a random base acceleration, modeled by a stationary filtered white noise process, in order to consider resonant effects. The main system is a SDF system, while structural frequency and damping, tuned mass ratio, filter main frequency and damping are affected by uncertainties. They are described by a mean value and a variance (standard deviation), assuming that they are all mutually statistically independent.

Assuming acceleration and displacement reduction as objective function, first ordinary CSSO is performed as a benchmark for the subsequent robust optimization process. The results show that the adopted OF significantly influences the performances, in particular for what concerns the number of dampers. Indeed,

the widening of the suppression band, due to an increase of the number of the dampers, may lead to undesired amplifications depending on the PSD system response. In detail, the displacement PSD for the adopted system shows a narrow band behavior that induces worse performances if the number of dampers increases. Instead, the PSD of absolute acceleration characterizes a broader band process. Therefore, a wider band of suppression improves the system response.

To perform the robust optimum design, mean and standard deviations of the deterministic OF are evaluated. Robustness is formulated as a MOOP, in which both the mean and the standard deviation are minimized. The results show a significant improvement in performance control and in the limitation of the OF dispersion, in comparison with standard conventional solutions. The MTMD demonstrated to be more robust than the single TMD, considering the previously tuning problems, also for the deterministic case. Considering the absolute acceleration, increasing the number of dampers is always positive. Conversely, for the displacements, it induces a loss of performance and sensitivity.

The following conclusions can be made:

- A deterministic optimization is inappropriate for sensible systems as TMDs, while a robust optimization aims to better control the results with low computational efforts;
- The adopted OF (displacement and absolute acceleration) influences significantly the optimal design parameters, depending on their PSD;
- Increasing the number of dampers leads to more robust designs because they act on a wider band of suppression. This is true until the in phase amplification, due to the wide band approach, becomes difficult to be controlled. This threshold depends on the bandwidth of the system response process. Therefore, the nature of the exciting action and the system have to be carefully considered within the optimization problems.

Overall, the choices depend on the required performances in terms of displacements and acceleration, coupled together with a necessary level of robustness.

However, an extended study about the influence of the soil nature, and/or the type of external action, on more samples, should be considered before generalization of such observations.

References

References

[1] L. D. Lutes, S. Sarkani, Random VIbrations: Analysis of Structural and Mechanical Systems, Elsevier Science, 2003.

[2] R. Rana, T. Soong, Parametric study and simplified design of tuned mass dampers, Engineering Structures 20 (3) (1998) 193–204.

[3] S. Elias, V. Matsagar, T. Datta, Distributed tuned mass dampers for multimode control of benchmark building under seismic excitations, Journal of Earthquake Engineering 23 (7) (2019) 1137–1172.

[4] F. Yang, R. Sedaghati, E. Esmailzadeh, Vibration suppression of structures using tuned mass damper technology: A state-of-the-art review, JVC/Journal of Vibration and Control 28 (7-8) (2022) 812–836.

[5] A. Ocak, S. Nigdeli, G. BekdaÅŸ, Passive control via mass dampers: A review of state-of-the-art developments, Studies in Systems, Decision and Control 432 (2022) 15–40.

[6] F. Ubertini, Prevention of suspension bridge flutter using multiple tuned mass dampers, Wind and Structures, An International Journal 13 (3) (2010) 235–256.

[7] S.-D. Kwon, K.-S. Park, Suppression of bridge flutter using tuned mass dampers based on robust performance design, Journal of Wind Engineering and Industrial Aerodynamics 92 (11) (2004) 919–934.

[8] L. Marian, A. Giaralis, Optimal design of a novel tuned mass-damper-inerter (tmdi) passive vibration control configuration for stochastically

support-excited structural systems, Probabilistic Engineering Mechanics 38 (2014) 156–164.

[9] Z. Wang, A. Giaralis, Enhanced motion control performance of the tuned mass damper inerter through primary structure shaping, Structural Control and Health Monitoring 28 (8).

[10] N. Nigam, Structural optimization in random vibration environment, American Institute of Aeronautics and Astronautics Journal 10 (4) (1972) 551–553.

[11] M. Constantinou, I. Tadjbakhsh, Optimum design of a first story damping system, Computers and Structures 17 (2) (1983) 305–310.

[12] I. Takewaki, An approach to stiffness-damping simultaneous optimization, Computer Methods in Applied Mechanics and Engineering 189 (2) (2000) 641–650.

[13] K.-S. Park, H.-M. Koh, D. Hahm, Integrated optimum design of viscoelastically damped structural systems, Engineering Structures 26 (5) (2004) 581–591.

[14] G. C. Marano, F. Trentadue, R. Greco, Optimum design criteria for elastic structures subject to random dynamic loads, Engineering Optimization 38 (7) (2006) 853–871.

[15] F. Rüdinger, Optimal vibration absorber with nonlinear viscous power law damping and white noise excitation, Journal of Engineering Mechanics 132 (1) (2006) 46–53.

[16] N. Hoang, P. Warnitchai, Design of multiple tuned mass dampers by using a numerical optimizer, Earthquake engineering & structural dynamics 34 (2) (2005) 125–144.

[17] G. Marano, F. Trentadue, B. Chiaia, Stochastic reliability based design criteria for linear structure subject to random vibrations, in: ASME 8th

Biennial Conference on Engineering Systems Design and Analysis, American Society of Mechanical Engineers Digital Collection, 2006, pp. 341–348.

[18] S. Chakraborty, B. K. Roy, Reliability based optimum design of tuned mass damper in seismic vibration control of structures with bounded uncertain parameters, Probabilistic Engineering Mechanics 26 (2) (2011) 215–221.

[19] A. Giaralis, A. Taflanidis, Optimal tuned mass-damper-inerter (tmdi) design for seismically excited mdof structures with model uncertainties based on reliability criteria, Structural Control and Health Monitoring 25 (2) (2018) e2082.

[20] D. Li, H. Tang, S. Xue, Robust design of tuned mass damper with hybrid uncertainty, Structural Control and Health Monitoring 28 (10) (2021) e2803.

[21] S. Elias, V. Matsagar, Research developments in vibration control of structures using passive tuned mass dampers, Annual Reviews in Control 44 (2017) 129–156.

[22] K. Bhowmik, N. Debnath, Stochastic design of multiple tuned mass damper system under seismic excitation, Archive of Applied Mechanics 92 (1) (2022) 383–404.

[23] T. Soong, G. Dargush, Passive energy dissipation systems in structural engineering wiley, Chichester, UK.

[24] M. Domaneschi, L. Martinelli, E. Po, Control of wind buffeting vibrations in a suspension bridge by tmd: Hybridization and robustness issues, Computers and Structures 155 (2015) 3–17.

[25] R. Husid, Características de terremotos. análisis general, Revista IDIEM 8 (1) (1969) ág–21.

[26] G. Muscolino, Dinamica delle strutture, McGraw-Hill, 2002.

[27] F. Zhang, The Schur Complement and its Applications, Springer, 2005.

[28] C. A. C. Coello, A comprehensive survey of evolutionary-based multiobjective optimization techniques, Knowledge and Information systems 1 (3) (1999) 269–308.

[29] D. Kalyanmoy, Multi-Objective Optimization using Evolutionary Algorithms, John Wiley & Sons, 2001.

[30] L. Zuo, S. A. Nayfeh, Optimization of the individual stiffness and damping parameters in multiple-tuned-mass damper systems, in: Smart Structures and Materials 2003: Damping and Isolation, Vol. 5052, SPIE, 2003, pp. 217–229.

[31] N. Hoang, P. Warnitchai, Design of multiple tuned mass dampers by using a numerical optimizer, Earthquake engineering & structural dynamics 34 (2) (2005) 125–144.

[32] M. Domaneschi, Feasible control solutions of the asce benchmark cable-stayed bridge, Structural Control & Health Monitoring 17 (2009) 675–693.

[33] G. C. Marano, S. Sgobba, R. Greco, M. Mezzina, Robust optimum design of tuned mass dampers devices in random vibrations mitigation, Journal of Sound and Vibration 313 (3-5) (2008) 472–492.

[34] R. Clough, P. J., Dynamics of structures, McGraw-Hill, 1993.

[35] G. C. Marano, R. Greco, G. Palombella, Stochastic optimum design of linear tuned mass dampers for seismic protection of high towers, Structural Engineering and Mechanics 29 (6) (2008) 603–622.

Appendix A. System matrices and their derivatives

The mechanical characteristics matrices of the dampers are:

$$\boldsymbol{M}_t = diag(\vec{\gamma}_t m_s) = \begin{bmatrix} m_1 & 0 & \dots & 0 \\ 0 & m_2 & 0 & \vdots \\ \vdots & & \ddots & 0 \\ 0 & \dots & 0 & m_n \end{bmatrix} \tag{A.1}$$

$$\boldsymbol{C}_t = \begin{bmatrix} c_1 & 0 & \dots & 0 \\ 0 & c_2 & 0 & \vdots \\ \vdots & & \ddots & 0 \\ 0 & \dots & 0 & c_n \end{bmatrix} \tag{A.2}$$

$$\boldsymbol{K}_t = \begin{bmatrix} k_1 & 0 & \dots & 0 \\ 0 & k_2 & 0 & \vdots \\ \vdots & & \ddots & 0 \\ 0 & \dots & 0 & k_n \end{bmatrix} \tag{A.3}$$

Appendix A.1. Protected case

The system matrix obtained from eq.(13) has the following form:

$$\bar{\boldsymbol{D}} = \begin{bmatrix} \boldsymbol{D}_N & \boldsymbol{D}_{Nf} \\ \boldsymbol{0} & \boldsymbol{D}_f \end{bmatrix}$$

In the protected case the system matrix of the SDF oscillator plus the tuned mass dampers is a $[2(1+n)] \times [2(1+n)]$ matrix (where n is the number of TMDs) of the following form:

$$\boldsymbol{D}_N = \begin{bmatrix} 0 & \dots & \dots & 0 & 1 & \dots & \dots & 0 \\ \vdots & \ddots & & \vdots & \vdots & \ddots & & \vdots \\ \vdots & & \ddots & \vdots & \vdots & & \ddots & \vdots \\ 0 & \dots & \dots & 0 & 0 & \dots & \dots & 1 \\ -\omega_1^2 & \dots & 0 & \omega_1^2 & -2\xi_1\omega_1 & \dots & 0 & 2\xi_1\omega_1 \\ \vdots & \ddots & \vdots & \vdots & \vdots & \ddots & \vdots & \vdots \\ 0 & \dots & -\omega_n^2 & \omega_n^2 & 0 & \dots & -2\xi_n\omega_n & 2\xi_n\omega_n \\ \gamma_1\cdot\omega_1^2 & \dots & \gamma_n\cdot\omega_n^2 & \omega_s^2+\sum_{i=1}^n \gamma_i\cdot\omega_i^2 & \gamma_1\cdot 2\xi_1\omega_1 & \dots & \gamma_n\cdot 2\xi_n\omega_n & 2\xi_s\omega_s+\sum_{i=1}^n \gamma_i\cdot 2\xi_i\omega_i \end{bmatrix}$$

The system matrix of the Tajimi-Kanai filter is a (2×2) matrix of this form:

$$\boldsymbol{D}_f = \boldsymbol{D}_K = \begin{bmatrix} 0 & 1 \\ -\omega_K^2 & -2\xi_K\omega_K \end{bmatrix}$$

The matrix $\boldsymbol{D}_{Nf}$, that indicates the influence of the filter on the system, is a $[(n+1)\times 2]$ rectangular matrix of the form:

$$\boldsymbol{D}_{Nf} = \begin{bmatrix} m_1^{-1}\cdot\omega_K^2 & m_1^{-1}\cdot 2\xi_K\omega_K \\ \vdots & \vdots \\ m_n^{-1}\cdot\omega_K^2 & m_n^{-1}\cdot 2\xi_K\omega_K \\ m_s^{-1}\cdot\omega_K^2 & m_s^{-1}\cdot 2\xi_K\omega_K \end{bmatrix}$$

The derivatives of the matrix $\bar{\boldsymbol{D}}$ respect to the i^{th} component d_i of the design parameters is calculated by derivation of the sub matrices that compose it:

$$(\bar{\boldsymbol{D}})_{d_i} = \begin{bmatrix} (\boldsymbol{D}_N)_{d_i} & (\boldsymbol{D}_{Nf})_{d_i} \\ \mathbf{0} & (\boldsymbol{D}_f)_{d_i} \end{bmatrix}$$

The derivatives respect each element of $\vec{d} = [\omega_s, \xi_s, \omega_K, \xi_K, \gamma_t]$ are reported below.

$$(\boldsymbol{D}_N)_{\omega_s} = \begin{bmatrix} 0 & \dots & \dots & 0 & 0 & \dots & \dots & 0 \\ \vdots & \ddots & & \vdots & \vdots & \ddots & & \vdots \\ \vdots & & \ddots & \vdots & \vdots & & \ddots & \vdots \\ 0 & \dots & \dots & 0 & 0 & \dots & \dots & 0 \\ 0 & \dots & 0 & 0 & 0 & \dots & 0 & 0 \\ \vdots & \ddots & \vdots & \vdots & \vdots & \ddots & \vdots & \vdots \\ 0 & \dots & 0 & 0 & 0 & \dots & 0 & 0 \\ 0 & \dots & 0 & 2\omega_s & 0 & \dots & 0 & 2\xi_s \end{bmatrix}$$

$$(\boldsymbol{D}_N)_{\xi_s} = \begin{bmatrix} 0 & \dots & \dots & 0 & 0 & \dots & \dots & 0 \\ \vdots & \ddots & & \vdots & \vdots & \ddots & & \vdots \\ \vdots & & \ddots & \vdots & \vdots & & \ddots & \vdots \\ 0 & \dots & \dots & 0 & 0 & \dots & \dots & 0 \\ 0 & \dots & 0 & 0 & 0 & \dots & 0 & 0 \\ \vdots & \ddots & \vdots & \vdots & \vdots & \ddots & \vdots & \vdots \\ 0 & \dots & 0 & 0 & 0 & \dots & 0 & 0 \\ 0 & \dots & 0 & 0 & 0 & \dots & 0 & 2\omega_s \end{bmatrix}$$

$$(\boldsymbol{D}_N)_{\omega_K} = \begin{bmatrix} 0 & \dots & \dots & 0 & 0 & \dots & \dots & 0 \\ \vdots & \ddots & & \vdots & \vdots & \ddots & & \vdots \\ \vdots & & \ddots & \vdots & \vdots & & \ddots & \vdots \\ 0 & \dots & \dots & 0 & 0 & \dots & \dots & 0 \\ 0 & \dots & 0 & 0 & 0 & \dots & 0 & 0 \\ \vdots & \ddots & \vdots & \vdots & \vdots & \ddots & \vdots & \vdots \\ 0 & \dots & 0 & 0 & 0 & \dots & 0 & 0 \\ 0 & \dots & 0 & 0 & 0 & \dots & 0 & 0 \end{bmatrix}$$

$$(\boldsymbol{D}_N)_{\xi_K} = \begin{bmatrix} 0 & \dots & \dots & 0 & 0 & \dots & \dots & 0 \\ \vdots & \ddots & & \vdots & \vdots & \ddots & & \vdots \\ \vdots & & \ddots & \vdots & \vdots & & \ddots & \vdots \\ 0 & \dots & \dots & 0 & 0 & \dots & \dots & 0 \\ 0 & \dots & 0 & 0 & 0 & \dots & 0 & 0 \\ \vdots & \ddots & \vdots & \vdots & \vdots & \ddots & \vdots & \vdots \\ 0 & \dots & 0 & 0 & 0 & \dots & 0 & 0 \\ 0 & \dots & 0 & 0 & 0 & \dots & 0 & 0 \end{bmatrix}$$

$$(\boldsymbol{D}_N)_{\gamma_t} = \begin{bmatrix} 0 & \dots & \dots & 0 & 0 & \dots & \dots & 0 \\ \vdots & \ddots & & \vdots & \vdots & \ddots & & \vdots \\ \vdots & & \ddots & \vdots & \vdots & & \ddots & \vdots \\ 0 & \dots & \dots & 0 & 0 & \dots & \dots & 0 \\ 0 & \dots & 0 & 0 & 0 & \dots & 0 & 0 \\ \vdots & \ddots & \vdots & \vdots & \vdots & \ddots & \vdots & \vdots \\ 0 & \dots & 0 & 0 & 0 & \dots & 0 & 0 \\ \omega_1^2 & \dots & \omega_n^2 & \sum_{i=1}^n \omega_i^2 & 2\xi_1\omega_1 & \dots & 2\xi_n\omega_n & \sum_{i=1}^n 2\xi_i\omega_i \end{bmatrix}$$

$$(\boldsymbol{D}_K)_{\omega_s} = \begin{bmatrix} 0 & 0 \\ 0 & 0 \end{bmatrix}, \quad (\boldsymbol{D}_K)_{\xi_s} = \begin{bmatrix} 0 & 0 \\ 0 & 0 \end{bmatrix}, \quad (\boldsymbol{D}_K)_{\omega_K} = \begin{bmatrix} 0 & 0 \\ 2\omega_K & 2\xi_K \end{bmatrix}$$

$$(\boldsymbol{D}_K)_{\xi_K} = \begin{bmatrix} 0 & 0 \\ 0 & 2\omega_K \end{bmatrix}, \qquad (\boldsymbol{D}_K)_{\gamma_t} = \begin{bmatrix} 0 & 0 \\ 0 & 0 \end{bmatrix}$$

$$(\boldsymbol{D}_{Nf})_{\omega_s} = \begin{bmatrix} 0 & 0 \\ \vdots & \vdots \\ 0 & 0 \\ 0 & 0 \end{bmatrix}, \quad (\boldsymbol{D}_{Nf})_{\xi_s} = \begin{bmatrix} 0 & 0 \\ \vdots & \vdots \\ 0 & 0 \\ 0 & 0 \end{bmatrix}, \quad (\boldsymbol{D}_{Nf})_{\omega_K} = \begin{bmatrix} m_1^{-1} \cdot 2\omega_K & m_1^{-1} \cdot 2\xi_K \\ \vdots & \vdots \\ m_n^{-1} \cdot 2\omega_K & m_n^{-1} \cdot 2\xi_K \\ m_s^{-1} \cdot 2\omega_K & m_s^{-1} \cdot 2\xi_K \end{bmatrix}$$

$$(\boldsymbol{D}_{Nf})_{\xi_K} = \begin{bmatrix} 0 & m_2^{-1} \cdot 2\omega_K \\ \vdots & \vdots \\ 0 & m_n^{-1} \cdot 2\omega_K \\ 0 & m_s^{-1} \cdot 2\omega_K \end{bmatrix} \qquad (\boldsymbol{D}_{Nf})_{\gamma_t} = \begin{bmatrix} 0 & 0 \\ \vdots & \vdots \\ 0 & 0 \\ 0 & 0 \end{bmatrix}$$

Appendix A.2. Unprotected case

In the unprotected case the system matrix has the following form:

$$\bar{\boldsymbol{D}}_0 = \begin{bmatrix} \boldsymbol{D}_{N,0} & \boldsymbol{D}_{Nf,0} \\ \boldsymbol{0} & \boldsymbol{D}_f \end{bmatrix}$$

The system matrix of the SDF oscillator is a 2×2 matrix of the following form:

$$\boldsymbol{D}_{N,0} = \begin{bmatrix} 0 & 1 \\ -\omega_s^2 & -2\xi_s\omega_s \end{bmatrix}$$

The system matrix of the Tajimi-Kanai filter does not change, it is a (2×2) matrix of this form:

$$\boldsymbol{D}_f = \boldsymbol{D}_K = \begin{bmatrix} 0 & 1 \\ -\omega_K^2 & -2\xi_K\omega_K \end{bmatrix}$$

The matrix $\boldsymbol{D}_{Nf,0}$ that indicates the influence of the filter on the system is a (1×2) rectangular matrix of the form:

$$\boldsymbol{D}_{Nf} = \begin{bmatrix} m_s^{-1} \cdot \omega_K^2 & m_s^{-1} \cdot 2\xi_K\omega_K \end{bmatrix}$$

The derivatives of the matrix $\bar{\boldsymbol{D}}_0$ respect to the component d_i of the design parameters is given by the derivation of the sub matrices that compose it:

$$(\bar{\boldsymbol{D}}_0)_{d_i} = \begin{bmatrix} (\boldsymbol{D}_{N,0})_{d_i} & (\boldsymbol{D}_{Nf,0})_{d_i} \\ \boldsymbol{0} & (\boldsymbol{D}_f)_{d_i} \end{bmatrix}$$

The derivatives respect each element of $\vec{d} = [\omega_s, \xi_s, \omega_K, \xi_K, \gamma_t]$ are reported below.

$$(\boldsymbol{D}_{N,0})_{\omega_s} = \begin{bmatrix} 0 & 0 \\ -2\omega_s & -2\xi_s \end{bmatrix}, \quad (\boldsymbol{D}_{N,0})_{\xi_s} = \begin{bmatrix} 0 & 0 \\ 0 & -2\omega_s \end{bmatrix}, \quad (\boldsymbol{D}_{N,0})_{\omega_K} = \begin{bmatrix} 0 & 0 \\ 0 & 0 \end{bmatrix}$$

$$(\boldsymbol{D}_{N,0})_{\xi_K} = \begin{bmatrix} 0 & 0 \\ 0 & 0 \end{bmatrix}, \qquad (\boldsymbol{D}_{N,0})_{\gamma_t} = \begin{bmatrix} 0 & 0 \\ 0 & 0 \end{bmatrix}$$

$$(\boldsymbol{D}_K)_{\omega_s} = \begin{bmatrix} 0 & 0 \\ 0 & 0 \end{bmatrix}, \quad (\boldsymbol{D}_K)_{\xi_s} = \begin{bmatrix} 0 & 0 \\ 0 & 0 \end{bmatrix}, \quad (\boldsymbol{D}_K)_{\omega_K} = \begin{bmatrix} 0 & 0 \\ 2\omega_K & 2\xi_K \end{bmatrix}$$

$$(\boldsymbol{D}_K)_{\xi_K} = \begin{bmatrix} 0 & 0 \\ 0 & 2\omega_K \end{bmatrix}, \qquad (\boldsymbol{D}_K)_{\gamma_t} = \begin{bmatrix} 0 & 0 \\ 0 & 0 \end{bmatrix}$$

$$(\boldsymbol{D}_{Nf,0})_{\omega_s} = \begin{bmatrix} 0 & 0 \end{bmatrix}, \quad (\boldsymbol{D}_{Nf,0})_{\xi_s} = \begin{bmatrix} 0 & 0 \end{bmatrix}, \quad (\boldsymbol{D}_{Nf,0})_{\omega_K} = \begin{bmatrix} m_s^{-1} \cdot 2\omega_K & m_s^{-1} \cdot 2\xi_K \end{bmatrix}$$

$$(\boldsymbol{D}_{Nf,0})_{\xi_K} = \begin{bmatrix} 0 & m_s^{-1} \cdot 2\omega_K \end{bmatrix}, \qquad (\boldsymbol{D}_{Nf,0})_{\gamma_t} = \begin{bmatrix} 0 & 0 \end{bmatrix}$$

Appendix B. Tabulated results

In this section of the appendix are reported the values assumed by the objective function for variable frequency ratio and number of dampers.

Deterministic OF_{displ} (-) values for different frequency ratio ψ (-) and number of dampers

ψ	**1**	**2**	**3**	**4**	**5**	**6**	**7**	**8**	**9**	**10**
0.20	0.95	1.48	1.99	2.62	3.32	4.08	5.01	5.54	6.30	7.03
0.40	0.67	0.76	0.96	1.84	2.42	3.06	2.00	2.29	4.94	4.72
0.60	0.64	0.69	0.75	0.85	0.97	1.12	1.27	1.45	1.61	1.78
0.80	0.61	0.66	0.69	0.74	0.80	0.88	0.97	1.08	1.18	1.29
1.00	0.63	0.68	0.71	0.74	0.79	0.85	0.92	0.99	1.07	1.16
1.20	0.69	0.75	0.79	0.83	0.88	0.93	1.00	1.08	1.16	1.25
1.40	0.77	0.84	0.88	0.93	0.99	1.06	1.14	1.22	1.31	1.41
1.60	0.84	0.91	0.96	1.02	1.09	1.18	1.26	1.38	1.47	1.59

Deterministic OF_{acc} (-) values for different frequency ratio ψ (-) and number of dampers

$\psi(-)$	**1**	**2**	**3**	**4**	**5**	**6**	**7**	**8**	**9**	**10**
0.20	0.66	1.21	1.98	2.84	2.85	3.77	4.44	5.00	7.39	6.73
0.40	0.44	0.37	0.33	0.33	0.39	0.51	0.63	0.80	1.02	1.14
0.60	0.42	0.35	0.30	0.28	0.26	0.24	0.23	0.22	0.23	0.24
0.80	0.41	0.33	0.29	0.26	0.24	0.22	0.28	0.20	0.32	0.19
1.00	0.42	0.35	0.30	0.27	0.25	0.23	0.22	0.21	0.20	0.20
1.20	0.47	0.40	0.35	0.32	0.30	0.28	0.26	0.25	0.24	0.23
1.40	0.54	0.47	0.42	0.39	0.36	0.34	0.32	0.31	0.30	0.29
1.60	0.59	0.54	0.49	0.46	0.43	0.49	0.39	0.37	0.35	0.35

OF_{displ} results for fixed damping ratio ξ_t (-) and varying tuning ratio ρ_t (-)

TMD	ξ_t	$\rho_{t,1}$	$\rho_{t,2}$	$\rho_{t,3}$	$\rho_{t,4}$	$\rho_{t,5}$	$\rho_{t,6}$	$\rho_{t,7}$	$\rho_{t,8}$	$\rho_{t,9}$	$\rho_{t,10}$	$\mu_{OF,displ}$
1	0.14	0.60	-	-	-	-	-	-	-	-	-	0.62
2	0.10	0.58	0.31	-	-	-	-	-	-	-	-	0.66
3	0.10	0.32	0.57	0.14	-	-	-	-	-	-	-	0.69
4	0.09	0.56	0.33	0.20	0.14	-	-	-	-	-	-	0.73
5	0.08	0.17	0.23	0.54	0.34	0.14	-	-	-	-	-	0.77
6	0.08	0.14	0.53	0.34	0.24	0.19	0.14	-	-	-	-	0.82
7	0.08	0.26	0.51	0.35	0.20	0.14	0.17	0.14	-	-	-	0.88
8	0.07	0.14	0.50	0.19	0.16	0.27	0.35	0.14	0.22	-	-	0.94
9	0.07	0.24	0.36	0.18	0.20	0.16	0.14	0.14	0.49	0.28	-	1.01
10	0.07	0.18	0.48	0.29	0.14	0.17	0.36	0.24	0.14	0.14	0.21	1.09

OF_{acc} results for fixed damping ratio ξ_t (-) and varying tuning ratio ρ_t (-)

TMD	ξ_t	$\rho_{t,1}$	$\rho_{t,2}$	$\rho_{t,3}$	$\rho_{t,4}$	$\rho_{t,5}$	$\rho_{t,6}$	$\rho_{t,7}$	$\rho_{t,8}$	$\rho_{t,9}$	$\rho_{t,10}$	$\mu_{OF,displ}$
1	0.07	0.68	-	-	-	-	-	-	-	-	-	0.41
2	0.05	0.61	0.49	-	-	-	-	-	-	-	-	0.33
3	0.03	0.41	0.47	0.56	-	-	-	-	-	-	-	0.29
4	0.03	0.35	0.52	0.45	0.40	-	-	-	-	-	-	0.26
5	0.03	0.43	0.38	0.50	0.31	0.34	-	-	-	-	-	0.25
6	0.02	0.37	0.41	0.34	0.47	0.28	0.31	-	-	-	-	0.23
7	0.02	0.26	0.33	0.30	0.36	0.28	0.44	0.39	-	-	-	0.21
8	0.02	0.43	0.32	0.24	0.38	0.28	0.26	0.35	0.30	-	-	0.20
9	0.02	0.41	0.27	0.23	0.29	0.24	0.26	0.37	0.31	0.34	-	0.20
10	0.02	0.24	0.21	0.27	0.33	0.31	0.23	0.40	0.25	0.36	0.29	0.19

Displacements robust optimization results for fixed damping ratio ξ_t (-) and varying tuning ratio ρ_t (-) (1 TMD). The row "det." corresponds to the optimal deterministic parameters.

Points	$\rho_t(-)$	$\xi_t(-)$	$\mu_{OF,displ}(-)$	$\sigma_{OF,displ}(-)$
(s)	0.55	0.20	0.73	0.04
(v)	0.14	0.14	0.96	0.01
(o)	0.44	0.31	0.82	0.03
(p)	0.14	0.10	0.97	0.01
(*)	0.48	0.29	0.80	0.03
(+)	0.55	0.21	0.73	0.04
(x)	0.49	0.27	0.79	0.03
det.	0.60	0.14	0.60	0.05

Displacements robust optimization results for fixed damping ratio ξ_t (-) and varying tuning ratio ρ_t (-) (2 TMDs). The row "det." corresponds to the optimal deterministic parameters.

Points	$\xi_t(-)$	$\rho_{t,1}(-)$	$\rho_{t,2}(-)$	$\mu_{OF,displ}(-)$	$\sigma_{OF,displ}(-)$
(s)	0.24	0.46	0.16	0.84	0.03
(v)	0.27	0.30	0.15	0.91	0.02
(o)	0.10	0.14	0.14	0.97	0.01
(p)	0.13	0.58	0.16	0.71	0.04
(*)	0.25	0.15	0.45	0.85	0.03
(+)	0.15	0.57	0.15	0.73	0.03
(x)	0.19	0.54	0.14	0.79	0.03
det.	0.10	0.58	0.31	0.66	0.05

Displacements robust optimization results for fixed damping ratio ξ_t (-) and varying tuning ratio ρ_t (-) (3 TMDs). The row "det." corresponds to the optimal deterministic parameters.

Points	ξ_t	$\rho_{t,1}(-)$	$\rho_{t,2}(-)$	$\rho_{t,3}(-)$	$\mu_{OF,displ}(-)$	$\sigma_{OF,displ}(-)$
(s)	0.09	0.57	0.14	0.33	0.03	0.71
(v)	0.21	0.15	0.22	0.15	0.02	0.94
(o)	0.13	0.24	0.14	0.55	0.01	0.75
(p)	0.21	0.15	0.15	0.27	0.04	0.93
(*)	0.21	0.14	0.14	0.42	0.03	0.88
(+)	0.20	0.14	0.15	0.47	0.03	0.85
(x)	0.19	0.14	0.21	0.15	0.03	0.95
det.	0.10	0.32	0.57	0.14	0.69	0.06

Acceleration robust optimization results for fixed damping ratio ξ_t (-) and varying tuning ratio ρ_t (-) (1 TMD). The row "det." corresponds to the optimal deterministic parameters.

Points	$\xi_t(-)$	$\rho_t(-)$	$\mu_{OF,acc}(-)$	$\sigma_{OF,acc}(-)$
(s)	0.14	0.17	0.95	0.01
(v)	0.15	0.12	0.96	0.01
(o)	0.67	0.09	0.45	0.02
(p)	0.19	0.40	0.91	0.02
(*)	0.67	0.06	0.43	0.03
(+)	0.14	0.22	0.94	0.01
(x)	0.67	0.07	0.43	0.02
det.	0.68	0.07	0.41	0.03

Acceleration robust optimization results for fixed damping ratio ξ_t (-) and varying tuning ratio ρ_t (-) (2 TMD). The row "det." corresponds to the optimal deterministic parameters.

Points	$\xi_t(-)$	$\rho_{t,1}(-)$	$\rho_{t,2}(-)$	$\mu_{OF,acc}(-)$	$\sigma_{OF,acc}(-)$
(s)	0.05	0.60	0.50	0.34	0.02
(v)	0.08	0.60	0.48	0.39	0.01
(o)	0.10	0.47	0.59	0.46	0.01
(p)	0.09	0.61	0.43	0.44	0.01
(*)	0.09	0.61	0.43	0.43	0.01
(+)	0.06	0.61	0.48	0.35	0.02
(x)	0.05	0.61	0.48	0.35	0.02
det.	0.05	0.61	0.49	0.34	0.03

Acceleration robust optimization results for fixed damping ratio ξ_t (-) and varying tuning ratio ρ_t (-) (3 TMD). The row "det." corresponds to the optimal deterministic parameters.

Points	$\xi_t(-)$	$\rho_{t,1}(-)$	$\rho_{t,2}(-)$	$\rho_{t,3}(-)$	$\mu_{OF,acc}(-)$	$\sigma_{OF,acc}(-)$
(s)	0.06	0.40	0.55	0.46	0.33	0.01
(v)	0.06	0.46	0.57	0.35	0.35	0.01
(o)	0.07	0.45	0.57	0.37	0.37	0.01
(p)	0.05	0.40	0.56	0.46	0.31	0.02
(*)	0.04	0.41	0.55	0.47	0.29	0.02
(+)	0.08	0.40	0.55	0.43	0.41	0.01
(x)	0.06	0.46	0.57	0.35	0.35	0.01
det.	0.03	0.41	0.47	0.56	0.29	0.03